AIP | The Journal of Chemical Physics

A spherical cavity model for quadrupolar dielectrics

Iglika M. Dimitrova, Radomir I. Slavchov, Tzanko Ivanov, and Sebastian Mosbach

Citation: The Journal of Chemical Physics **144**, 114502 (2016); doi: 10.1063/1.4943196
View online: http://dx.doi.org/10.1063/1.4943196
View Table of Contents: http://scitation.aip.org/content/aip/journal/jcp/144/11?ver=pdfcov
Published by the AIP Publishing

A spherical cavity model for quadrupolar dielectrics

Iglika M. Dimitrova,[1] Radomir I. Slavchov,[1,2,a)] Tzanko Ivanov,[3] and Sebastian Mosbach[2]
[1]*Department of Physical Chemistry, Faculty of Chemistry and Pharmacy, Sofia University, 1164 Sofia, Bulgaria*
[2]*Department of Chemical Engineering and Biotechnology, Cambridge University, CB2 3RA Cambridge, United Kingdom*
[3]*Department of Theoretical Physics, Faculty of Physics, Sofia University, 1164 Sofia, Bulgaria*

(Received 2 December 2015; accepted 22 February 2016; published online 17 March 2016)

The dielectric properties of a fluid composed of molecules possessing both dipole and quadrupole moments are studied based on a model of the Onsager type (molecule in the centre of a spherical cavity). The dielectric permittivity ε and the macroscopic quadrupole polarizability α_Q of the fluid are related to the basic molecular characteristics (molecular dipole, polarizability, quadrupole, quadrupolarizability). The effect of α_Q is to increase the reaction field, to bring forth reaction field gradient, to decrease the cavity field, and to bring forth cavity field gradient. The effects from the quadrupole terms are significant in the case of small cavity size in a non-polar liquid. The quadrupoles in the medium are shown to have a small but measurable effect on the dielectric permittivity of several liquids (Ar, Kr, Xe, CH_4, N_2, CO_2, CS_2, C_6H_6, H_2O, CH_3OH). The theory is used to calculate the macroscopic quadrupolarizabilities of these fluids as functions of pressure and temperature. The cavity radii are also determined for these liquids, and it is shown that they are functions of density only. This extension of Onsager's theory will be important for non-polar solutions (fuel, crude oil, liquid CO_2), especially at increased pressures. © *2016 AIP Publishing LLC.* [http://dx.doi.org/10.1063/1.4943196]

I. INTRODUCTION

The macroscopic Poisson equation of electrostatics involves only the dipolar contribution to the dielectric displacement field, whereas quadrupole, octupole, etc., terms are neglected.[1,2] The absence of the quadrupole contribution in the macroscopic Maxwell equations is equivalent to neglect of the interaction of the electric field gradient with matter. When electric field $\boldsymbol{E}$ acts on a body, the body acquires dipole moment; the resulting macroscopic dipole moment density $\boldsymbol{P}$ (the polarization vector) is related to the field as $\boldsymbol{P} = \alpha_P \boldsymbol{E}$, where $\alpha_P = \varepsilon - \varepsilon_0$ is the polarizability of the medium. Similarly, the electric field gradient $\nabla \boldsymbol{E}$ induces a macroscopic quadrupole moment of density $\mathbf{Q}$ (the *quadrupolarization* tensor), proportional to $\nabla \boldsymbol{E}$, with proportionality coefficient α_Q, known either as the *quadrupolarizability*[3,4] or the *quadrupole polarizability*[5] of the medium (a tensor, in general). The quadrupolarizability is a basic characteristic of every solvent that has been shown to play a role in diverse phenomena such as solubility of polar molecules in non-polar solvents,[6,7] solvatochromism,[8] partition coefficients of electrolytes,[9] activity of dissolved electrolytes,[10] and the surface tension and the dipole moment of the interface between insulators.[11]

The value of the static macroscopic quadrupole polarizability is unknown even for common solvents because the macroscopic quadrupolarizability is hard to measure directly.[7,12] Two approaches for determination of α_Q exist. The first approach utilizes the effects of α_Q on various measurable properties of a solvent or a solute. The comparison between experimental data for these properties and theoretical results for the effects of the quadrupolarizability allows the value of α_Q to be determined. For example, the analysis of data for the partial molar properties and activity of dissolved ions allowed us to estimate α_Q of water, methanol, and other solvents.[9,10] This approach relies on the accuracy of the theoretical results for the respective effect. However, the underlying theory contains approximations and neglects numerous possibly significant effects,[9,10] which makes the obtained values of the quadrupole polarizability unreliable in the absence of independent validation.

A second approach is to relate α_Q to the molecular characteristics and calculate it theoretically. An ideal gas of concentration C made of molecules of mean molecular quadrupolarizability[13,7] α_q and permanent quadrupole moment $\mathbf{q}_0$ has the following macroscopic quadrupole polarizability:[7,9]

$$\alpha_Q = C\left(\alpha_q + \mathbf{q}_0{:}\mathbf{q}_0/10k_BT\right); \tag{1}$$

here T is temperature, k_B is the Boltzmann constant, and $\boldsymbol{A}{:}\boldsymbol{B} = A_{ij}B_{ji}$. This equation is analogous to the classical formula for the polarizability of a dilute gas, $\alpha_P = C(\alpha_p + \boldsymbol{p}_0 \cdot \boldsymbol{p}_0/3k_BT)$, where α_p is the mean molecular polarizability and $\boldsymbol{p}_0$ is the permanent dipole moment. However, Eq. (1) is inapplicable to dense fluids while α_Q is important for dense matter only. By analogy with the formula for α_P (which underestimates the value of α_P for polar liquids by a factor of 2-3), it can be expected that a dense fluid will have quadrupolarizability which is several times greater than the one predicted from Eq. (1).

Due to these problems, currently we do not dispose with trustworthy quadrupolarizabilities for any liquid of

a)E-mail: ris26@cam.ac.uk

interest. Both the approaches, outlined above, lead to, at best, crude estimates of the quadrupole polarizability. For example, the gas formula (1) yields values of the order of 1×10^{-30} F m for α_Q of water and methanol at normal conditions. With methanol,[10] the magnitude of the quadrupolarizability found from experimental activity of dissolved ions is $\alpha_Q \sim 10 \times 10^{-30}$ F m, which is acceptable in comparison with the "gaseous" value (few times higher, as expected). For water, however, the first approach leads to quadrupolarizability on the order of[9,10] 100×10^{-30} F m, compared to 1×10^{-30} F m according to Eq. (1)—such a discrepancy (two orders of magnitude) obviously poses a question mark on both estimates.

In view of this introduction, we can formulate the main aim of this work as follows: devise an approach to accurately predict the quadrupole polarizability α_Q of simple solvents using molecular data for $\boldsymbol{p}_0$, α_p, $\mathbf{q}_0$, and α_q. Towards this aim, we will generalize the classical Onsager model[14] of polar dielectrics and apply the generalized theory to a fluid made of molecules possessing quadrupole moment and quadrupolarizability. As we will show, this new theory allows the prediction of α_Q whenever ε, C, and the molecular properties of the solvent are known. We will use it to calculate the quadrupole polarizability α_Q as a function of temperature and pressure for several liquids of different complexity.

Apart from the main aim, the generalization of Onsager's model to quadrupolarizable media has value on its own. The chemistry of polar species dissolved in non-polar or weakly polar medium is governed by Onsager's reaction field.[15–18] Onsager's reaction field also forms the foundation of the theory of solvatochromism,[19,8] solvent effects on chemical equilibria,[20–22] and on kinetic rate constants.[23–25] Onsager's theory is based on a macroscopic model for the interaction between *solute dipole* and *solvent dipoles*. Numerous electrostatic models exist that generalize Onsager's theory by accounting also for the *solute quadrupole-solvent dipole* interactions,[15–17,21,26,27] and they have wide applications. What these models miss is the *solute dipole-solvent quadrupole* interaction, which is of the same order of magnitude.[28] The typical energy per dissolved molecule corresponding to this interaction can be estimated at several k_BT, and it must have a first order contribution to problems as important as the solvent ability of crude oil, fuel, and lubricants, especially under increased pressures. The reason for the "oversight" of the solute dipole-solvent quadrupole interaction is not physical but technical—the conventional Maxwell macroscopic equations neglect the quadrupolar properties of the medium which complicates the determination of this important solvent effect within the standard macroscopic theory. Some efforts were made[6,7] to formulate a continuum theory to describe solvation in quadrupolar solvents, such as benzene and supercritical CO_2. Chitanvis[6] attempted to find *the reaction field gradient* within a macroscopic theory. The quadrupolar solvatochromism[29] was considered macroscopically by Jeon and Kim.[8] Molecular level description is, in fact, well ahead of the classical macroscopic description of quadrupolar fluids—the perturbation theory,[28–30] the integral equation,[31–33] and the molecular dynamics[34–36] microscopic approaches have been applied successfully to quadrupolar liquids. Yet, even with the microscopic approach, the molecular quadrupolarizability has been neglected. This makes the continuum description a necessary step toward the "conquest" of the quadrupolar liquids.

A. Quadrupolar electrostatics

Let us first summarize our general approach to the electrostatics of quadrupolar media[9] and some relevant results obtained previously. Coulomb's macroscopic law of electrostatics reads

$$\nabla \cdot \boldsymbol{D} = \rho, \tag{2}$$

where ρ is the free charge density and $\boldsymbol{D}$ is electric displacement field. In quadrupolarizable media, the displacement field involves the contributions of both the dipole density ($\varepsilon_0 \boldsymbol{E} + \boldsymbol{P} = \varepsilon \boldsymbol{E}$) and[2] the tensor of the quadrupole moment density $\mathbf{Q}$,

$$\boldsymbol{D} = \varepsilon \boldsymbol{E} - \frac{1}{2} \nabla \cdot \mathbf{Q}. \tag{3}$$

Note that the numerical coefficient 1/2 in this equation depends on the choice of definition of quadrupole moment[9,15] (according to the one used here, a molecule of charge distribution ρ_{molecule} has molecular quadrupole $\mathbf{q} = \int (\boldsymbol{rr} - \mathbf{U}r^2/3)\rho_{\text{molecule}} d\boldsymbol{r}$, integrated over the volume of the molecule, where $\mathbf{U}$ is the unit tensor). In the derivation of Eq. (3), it is assumed that $\mathbf{Q}$ has a zero trace.[9] This excludes[11] the so-called Bethe contribution from the mean macroscopic potential, which stems mainly from the electrostatic potential of the atomic nuclei screened by their electronic clouds[36] and must be considered a component of the short-range steric interactions. A discussion of the mean potential stemming from Tr$\mathbf{Q}$ is provided in Refs. 7 and 11.

A constitutive relation between the quadrupole moment density and electric field gradient is required for the utilization of Eqs. (2) and (3). In Ref. 9, the following equation of state was derived for a gas in electrostatic field:

$$\mathbf{Q} = \alpha_Q \left(\nabla \boldsymbol{E} - \mathbf{U} \nabla \cdot \boldsymbol{E}/3 \right). \tag{4}$$

Other constitutive relations have been proposed in the literature,[6,7] which, however, involve non-zero trace. By substituting Eqs. (3) and (4) into Eq. (2) and using Ampère's law ($\boldsymbol{E} = -\nabla \phi$), one obtains the explicit form of the *electrostatic Coulomb-Ampère law in quadrupolarizable medium*,

$$\nabla^2 \phi - L_Q^2 \nabla^4 \phi = -\rho/\varepsilon. \tag{5}$$

Here, *the quadrupolar length* L_Q is defined with

$$L_Q^2 = \alpha_Q / 3\varepsilon. \tag{6}$$

The quadrupolar length is measuring the relative quadrupolar (α_Q) and polar (ε) strengths in a medium. The quantity L_Q is analogous to the Debye length[11] (measuring the ratio between the polar and ionic strengths in a medium). At $L_Q = 0$, the quadrupolar Coulomb-Ampère law (5) simplifies to Poisson's standard electrostatic equation,

$$\nabla^2 \phi = -\rho/\varepsilon. \tag{7}$$

Qualitatively, the effect from the quadrupolarizability of the medium is to damp the field gradient in the system[9–11] and to make the potential smoother. High fields are generally suppressed with the increase of L_Q.

Eq. (5) is a fourth-order differential equation. It therefore requires additional boundary conditions in comparison with Poisson's second-order Equation (7). The set of boundary conditions were derived only recently.[11,2,37,38,9] The boundary conditions that we need here refer to the spherical boundary between an empty cavity of radius $R_{\rm cav}$ and a quadrupolar medium and they are given as follows:

$$\begin{aligned} D_r(r = R_{\rm cav} - 0) &= D_r(r = R_{\rm cav} + 0), \\ Q_{rr}(r = R_{\rm cav} - 0) &= Q_{rr}(r = R_{\rm cav} + 0), \\ \phi(r = R_{\rm cav} - 0) &= \phi(r = R_{\rm cav} + 0). \end{aligned} \tag{8}$$

When the boundary surface is between two quadrupolar media, a fourth condition for continuity of the field must be fulfilled; for the boundary between one quadrupolarizable and one non-quadrupolarizable medium (investigated in this work), the field is discontinuous and a fourth condition is not required.[11]

Several basic electrostatic problems were investigated previously[9–11,38] within the frame of the quadrupolar Coulomb-Ampère law (5). A result relevant to this work is the one for the potential ϕ_e of a point charge e in a quadrupolarizable medium, which was found to be

$$\phi_e = \frac{e}{4\pi\varepsilon}\frac{1 - \exp(-r/L_Q)}{r}. \tag{9}$$

A striking feature of this potential is[9,6] that it is finite at $r = 0$ (where its value is $e/4\pi\varepsilon L_Q$). The point charge has, therefore, a finite self-energy $u_e = e^2/8\pi\varepsilon L_Q$. Such *regularization of the potential* is characteristic of quadrupolar electrostatics compared to what follows from Poisson's equation.[11,9] Another relevant problem analyzed in Ref. 9 was the one for a charge e placed inside an empty cavity in a medium of dielectric permittivity ε and quadrupolar length $L_Q = (\alpha_Q/3\varepsilon)^{1/2}$, i.e., we solved the problem for the Born energy u_e of an ion in a quadrupolar medium. The solution of Eqs. (5) and (8) for the *reaction potential* acting on the ion is given as follows:[9]

$$\phi_{\rm react} = -X_e e; \quad X_e = \frac{1}{4\pi R_{\rm cav}\varepsilon_0}\frac{\varepsilon - f_e\varepsilon_0}{\varepsilon}, \tag{10}$$

where the quadrupolar factor f_e stands for

$$f_e = \frac{1 + 3\frac{L_Q}{R_{\rm cav}}}{1 + 3\frac{L_Q}{R_{\rm cav}} + 3\frac{L_Q^2}{R_{\rm cav}^2}} \tag{11}$$

and $u_e = e\phi_{\rm react}/2$. At $L_Q = 0$, the correction factor f_e becomes equal to one and the expression (10) simplifies to the classical formula of Born.[39] The other limit, $L_Q \gg R_{\rm cav}$, coincides with the point charge self-energy above. In purely quadrupolar solvent made of permanent quadrupoles[30] ($\boldsymbol{p}_0 = \alpha_p = \alpha_q = 0$; $\varepsilon = \varepsilon_0$), under the condition that $L_Q \ll R_{\rm cav}$, from Eqs. (11), (6), and (1), one can obtain

$$u_e \approx -\frac{3L_Q^2 e^2}{8\pi\varepsilon_0 R_{\rm cav}^3} = -\frac{\alpha_Q e^2}{8\pi\varepsilon_0^2 R_{\rm cav}^3} \approx -\frac{e^2}{80\pi\varepsilon_0^2 R_{\rm cav}^3}\frac{C\mathbf{q}_0{:}\mathbf{q}_0}{k_{\rm B}T}. \tag{12}$$

This result was obtained previously as the continuum limit of the microscopic perturbation theory (Eq. (44) of Milischuk and Matyushov[30] with $(\sigma_0 + \sigma)/2 \equiv R_{\rm cav}$). This coincidence gives us additional confidence in our equation of state (4) and boundary conditions (8) (compare to Refs. 6 and 7).

In this work, we will analyze the related problems for the *reaction field* $\boldsymbol{E}_{\rm react}$ acting on a dipole in a quadrupolar medium and the *reaction field gradient* $\nabla\boldsymbol{E}_{\rm react}$ acting on a quadrupole in a quadrupolar medium (Sec. II A), within Onsager's spherical cavity model. In Sec. II B, we solve the problem for the *cavity field* $\boldsymbol{E}_{\rm cav}$ and the *cavity field gradient* $\nabla\boldsymbol{E}_{\rm cav}$ inside a cavity in a quadrupolar insulator placed in an external field, which is the second component of Onsager's theory of the dielectric permittivity of fluids. Onsager's famous equation for ε is generalized in Secs. II C and II D to quadrupolar fluids, and a similar formula for the macroscopic quadrupole polarizability α_Q is derived.

In Sec. III, the theoretical results are utilized to predict the quadrupolarizability as a function of pressure and temperature for the following fluids: Ar, Kr, Xe, CH_4 (of zero $\boldsymbol{p}_0$ and $\mathbf{q}_0$ but non-zero α_p and α_q), N_2, CO_2, CS_2, C_6H_6 (zero $\boldsymbol{p}_0$), H_2O, and CH_3OH. This choice of liquids is, on the one hand, for the sake of illustrating our approach on molecules of qualitatively and quantitatively different electric properties. On the other hand, there are previous estimations of the quadrupole polarizability of water and methanol.[9,10] Finally, the results for the liquid CH_4, C_6H_6, and CH_3OH are the first step toward the development and parameterization of a cavity model for solutions of polar molecules in fuels and lubricants, which are perhaps the most important examples of quadrupolar solvents in practice.

II. INTRODUCING QUADRUPOLES IN ONSAGER'S THEORY

In this section, we generalize Onsager's model to quadrupolar media. The macroscopic approach towards the quadrupolar properties of a medium was investigated previously by Chitanvis[6] and Jeon and Kim,[7,8] who obtained, however, results very different from those we present below due to their different boundary conditions and different constitutive relation for $\mathbf{Q}$ (cf. the discussion in Refs. 9 and 11).

A. Reaction field of a dipole and a quadrupole

A point dipole $\boldsymbol{p}$ (comprising permanent and induced components) is located in the centre of a spherical cavity (permittivity ε_0, zero quadrupolar length) of radius $R_{\rm cav}$ inside a medium of dielectric permittivity ε and quadrupolar length L_Q (Fig. 1(a)). To find the field of this dipole, we solve the quadrupolar Coulomb-Ampère equation (5) with boundary conditions (8) and with ρ being given by $-\boldsymbol{p}\cdot\nabla\delta(\boldsymbol{r})$, where $\delta(\boldsymbol{r}) \equiv \delta(x)\delta(y)\delta(z)$ is the 3-dimensional Dirac delta function. Field is absent at $\boldsymbol{r} \to \infty$. The solution of this problem for the potential ϕ_{p0} inside the cavity ($r < R_{\rm cav}$) is given by

$$\phi_{p0} = \frac{\boldsymbol{p}\cdot\boldsymbol{r}}{4\pi\varepsilon_0 r^3} - \boldsymbol{E}_{\rm react}\cdot\boldsymbol{r} \tag{13}$$

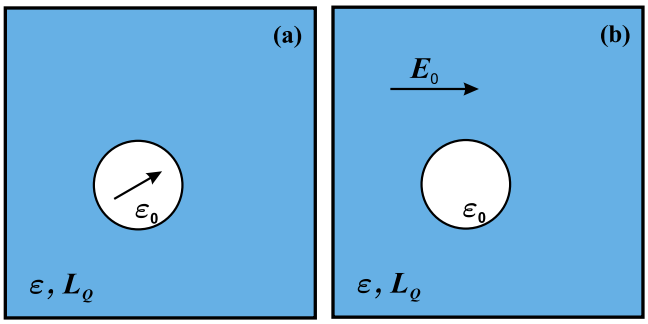

FIG. 1. (a) Dipole in a cavity in a quadrupolar medium. (b) Cavity in an external field.

and the potential ϕ_p outside the cavity ($r > R_{\rm cav}$) is

$$\phi_p = \frac{\boldsymbol{p}_{\rm ext}\cdot\boldsymbol{r}}{4\pi\varepsilon r^3}\left(1 - 9f_p\frac{L_Q^2}{R_{\rm cav}^2}\frac{r+L_Q}{R_{\rm cav}+4L_Q}\mathrm{e}^{-\frac{r-R_{\rm cav}}{L_Q}}\right). \quad (14)$$

Here $\boldsymbol{E}_{\rm react}$ is the *reaction field*[14] produced inside the cavity by the polarized medium, and is given by

$$\boldsymbol{E}_{\rm react} = X_p\boldsymbol{p}, \quad X_p = \frac{1}{2\pi\varepsilon_0 R_{\rm cav}^3}\frac{\varepsilon - f_p\varepsilon_0}{2\varepsilon + f_p\varepsilon_0}. \quad (15)$$

The *external dipole moment* $\boldsymbol{p}_{\rm ext}$ in Eq. (14) is the total dipole moment of the central molecule and its polarized surrounding and is given by the expression

$$\boldsymbol{p}_{\rm ext} = \frac{3\varepsilon}{2\varepsilon + f_p\varepsilon_0}\boldsymbol{p}. \quad (16)$$

The quardupolar factor f_p in the formulae above stands for the expression

$$f_p = \frac{1 + 4\frac{L_Q}{R_{\rm cav}}}{1 + 4\frac{L_Q}{R_{\rm cav}} + 9\frac{L_Q^2}{R_{\rm cav}^2} + 9\frac{L_Q^3}{R_{\rm cav}^3}}. \quad (17)$$

Eqs. (15) and (17) are analogous to the results (10) and (11) for a point charge in a cavity. The factor f_p is always smaller than 1. If the quadrupolarizability of the medium is negligible so that $L_Q \ll R_{\rm cav}$, then the maximal value $f_p = 1$ is reached and the results (15) and (16) for the external dipole moment and the reaction field simplify to the known equations of Onsager.[14] The quadrupolar correction is important for small species ($R_{\rm cav} \sim L_Q$) in fluids of low ε (when $\varepsilon \gg \varepsilon_0$, the L_Q-containing term $f_p\varepsilon_0$ in Eqs. (15) and (16) is negligible). According to Eq. (15), the reaction field increases with L_Q—an effect stemming from the additional attractive interaction between the central dipole and the medium quadrupoles (in full agreement with the critical remarks of Matyushov and Voth[28] on previous models). The reaction field in the spherical cavity has zero gradient and therefore it does not interact with the quadrupole moment of the central molecule (this allows us to investigate the medium reaction to the dipole and the quadrupole separately).

From Eqs. (15), (6), and (1), we can calculate the energy of interaction of a permanent dipole (i.e., $\boldsymbol{p} = \boldsymbol{p}_0$) with the medium in the limit $\varepsilon = \varepsilon_0$, $R_{\rm cav} \gg L_Q$ and $\alpha_p = \alpha_q = 0$,

$$u_p = -\frac{X_p p_0^2}{2} \approx -\frac{9L_Q^2 p_0^2}{4\pi\varepsilon_0 R_{\rm cav}^5} = -\frac{3p_0^2}{40\pi\varepsilon_0^2 R_{\rm cav}^5}\frac{C\mathbf{q}_0{:}\mathbf{q}_0}{k_{\rm B}T}. \quad (18)$$

This result is analogous to the energy (12) of a point charge in a medium made of solid quadrupoles. The expression coincides with the continuum single particle limit of the perturbation theory of Milischuk and Matyushov (Eq. (49) in Ref. 30 with $(\sigma_0 + \sigma)/2 \equiv R_{\rm cav}$), which is another confirmation of the theoretical framework exposed in Sec. I A.

Let us also discuss briefly the solution for the field of a *point dipole in quadrupolar medium in the absence of a cavity*. It can be obtained either from Eq. (14) by setting $\boldsymbol{p}_{\rm ext} = \boldsymbol{p}$ and $R_{\rm cav} \to 0$ or from the point charge formula (9) using the general relation $\phi_p = -\boldsymbol{p}\cdot\nabla\phi_e/e$. The result is

$$\phi_p = \frac{\boldsymbol{p}\cdot\boldsymbol{r}}{4\pi\varepsilon r^3}\left(1 - \frac{r+L_Q}{L_Q}\mathrm{e}^{-r/L_Q}\right). \quad (19)$$

This potential is finite, but not continuous. It is illustrated in Fig. 2.

Let us now consider the problem for the reaction field gradient of a *quadrupole* of magnitude $\mathbf{q}$ inside a spherical cavity. We solve the same equations but this time with $\rho = {}^1\!/_2\mathbf{q}{:}\nabla\nabla\delta(\boldsymbol{r})$. The potential ϕ_{q0} inside the cavity (at $r < R_{\rm cav}$) is (cf. Section A of the supplementary material[93])

$$\phi_{q0} = \frac{3\boldsymbol{r}\cdot\mathbf{q}\cdot\boldsymbol{r}}{8\pi\varepsilon_0 r^5} - \frac{1}{2}\boldsymbol{r}\cdot(\nabla\boldsymbol{E})_{\rm react}\cdot\boldsymbol{r}, \quad (20)$$

and the solution ϕ_q at $r > R_{\rm cav}$ is

$$\phi_q = \frac{3\boldsymbol{r}\cdot\mathbf{q}_{\rm ext}\cdot\boldsymbol{r}}{8\pi\varepsilon r^5}\left(1 - 18g_q\frac{r^2 + 3rL_Q + 3L_Q^2}{R_{\rm cav}^2}\mathrm{e}^{-\frac{r-R_{\rm cav}}{L_Q}}\right). \quad (21)$$

Here, the *reaction field gradient* $(\nabla\boldsymbol{E})_{\rm react}$ is given by the expression

$$(\nabla\boldsymbol{E})_{\rm react} = X_q\mathbf{q}, \quad X_q = \frac{9}{4\pi\varepsilon_0 R_{\rm cav}^5}\frac{\varepsilon - f_q\varepsilon_0}{3\varepsilon + 2f_q\varepsilon_0}, \quad (22)$$

and the *external quadrupole moment* $\mathbf{q}_{\rm ext}$ (the total quadrupole of the central molecule and the quadrupolarized surrounding

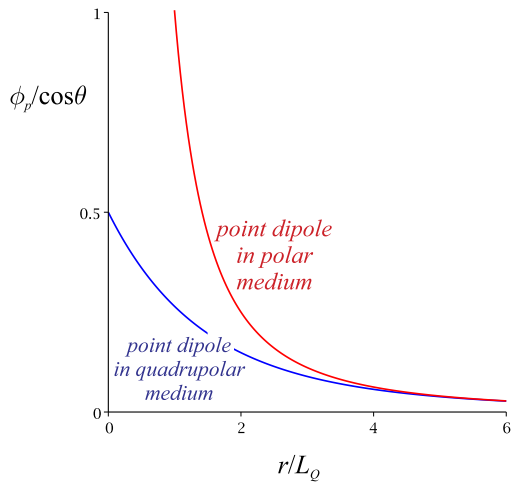

FIG. 2. The radial component of the potential of a point dipole in dipolar (red) and quadrupolar (blue) medium, according to Eq. (19), made dimensionless by setting $p = 4\pi\varepsilon L_Q^2$. In dipolar medium, the radial component is $1/r^2$ and is singular; in the quadrupolar one, the potential is finite.

medium) is

$$\mathbf{q}_{\text{ext}} = \frac{5\varepsilon}{3\varepsilon + 2f_q\varepsilon_0}\mathbf{q}. \tag{23}$$

The two quadrupolar factors f_q and g_q are given by the formulae

$$\begin{aligned} f_q &= \frac{1 + 6\frac{L_Q}{R_{\text{cav}}} + 6\left(\frac{L_Q}{R_{\text{cav}}}\right)^2}{1 + 6\frac{L_Q}{R_{\text{cav}}} + 24\left(\frac{L_Q}{R_{\text{cav}}}\right)^2 + 54\left(\frac{L_Q}{R_{\text{cav}}}\right)^3 + 54\left(\frac{L_Q}{R_{\text{cav}}}\right)^4}, \\ g_q &= \frac{\left(\frac{L_Q}{R_{\text{cav}}}\right)^2}{1 + 6\frac{L_Q}{R_{\text{cav}}} + 24\left(\frac{L_Q}{R_{\text{cav}}}\right)^2 + 54\left(\frac{L_Q}{R_{\text{cav}}}\right)^3 + 54\left(\frac{L_Q}{R_{\text{cav}}}\right)^4}. \end{aligned} \tag{24}$$

These results are similar to the respective Equations (15)-(17) for dipole. In the absence of medium quadrupole polarizability ($f_q = 1$), the reaction field gradient (22) simplifies to the one of Buckingham.[40]

A *point quadrupole* (no cavity) in a quadrupole medium creates the potential distribution,

$$\phi_q = \frac{3\boldsymbol{r}\cdot\mathbf{q}\cdot\boldsymbol{r}}{8\pi\varepsilon r^5}\left(1 - \frac{r^2 + 3rL_Q + 3L_Q^2}{3L_Q^2}\mathrm{e}^{-r/L_Q}\right). \tag{25}$$

This result can be obtained from Eq. (21) by setting $\mathbf{q}_{\text{ext}} = \mathbf{q}$ and $R_{\text{cav}} \to 0$, or from the point charge formula (9) using $\phi_q = \mathbf{q}{:}\nabla\nabla\phi_e/e$. The potential ϕ_q has a singularity at $r = 0$.

We can summarize the three results that we obtained for point sources ($R_{\text{cav}} = 0$) in a quadrupolar medium as follows. The potential of a point charge in a dipolar medium has $1/r$ singularity at $r = 0$, while it is finite and continuous in quadrupolar medium, Eq. (9). The point dipole classically has a $\phi \sim 1/r^2$ singularity in dipolar medium, while in quadrupolar, it has a finite (but discontinuous) potential, Eq. (19). Finally, the potential of a point quadrupole has a $1/r^3$ singularity in a dipolar and $1/r$ singularity in a quadrupolar medium. It is easy to predict that if octupolarizability is allowed in the medium, not only the potential but also the field of a point dipole will be finite and continuous, and thus the self-energy $-\boldsymbol{p}\cdot\boldsymbol{E}(0)$ of a dipole in an octupolar medium must be finite. A point quadrupole in octupolar medium will have a finite continuous potential but singular $\nabla\boldsymbol{E}$ and infinite self-energy; higher-order macroscopic multipolarizability will lead to additional regularization.

B. Cavity field and cavity field gradient

The second sub-model involved in Onsager's theory is the problem for a cavity in a continuum polarized by an external field $\boldsymbol{E}_0$ (Fig. 1(b)). Here, we generalize this problem for quadrupolar medium by using the quadrupolar electrostatic equations (5) and (8) instead of the conventional Poisson equation (in addition, we require $-\nabla\phi = \boldsymbol{E}_0$ at $r \to \infty$ and at $r \to 0$, the potential must be finite). The solution of this problem for the potential distribution ϕ_{E0} at $r < R_{\text{cav}}$ reads

$$\phi_{E0} = -\boldsymbol{E}_{\text{cav}}\cdot\boldsymbol{r}; \tag{26}$$

the potential ϕ_E at $r > R_{\text{cav}}$ is

$$\phi_E = -\boldsymbol{E}_0\cdot\boldsymbol{r} + \frac{\boldsymbol{p}_{\text{ext},E}\cdot\boldsymbol{r}}{4\pi\varepsilon r^3}\left(1 - 9f_p\frac{L_Q^2}{R_{\text{cav}}^2}\frac{r + L_Q}{R_{\text{cav}} + 4L_Q}\mathrm{e}^{-\frac{r-R_{\text{cav}}}{L_Q}}\right). \tag{27}$$

Here, the cavity field $\boldsymbol{E}_{\text{cav}}$ is proportional to the outer field $\boldsymbol{E}_0$,

$$\boldsymbol{E}_{\text{cav}} = Y_E\boldsymbol{E}_0, \quad Y_E = \frac{3f_E\varepsilon}{2\varepsilon + f_p\varepsilon_0}. \tag{28}$$

The moment $\boldsymbol{p}_{\text{ext},E}$ in Eq. (27) is the excess dipole moment of the cavity induced by the external field and is given by

$$\boldsymbol{p}_{\text{ext},E} = -4\pi\varepsilon R_{\text{cav}}^3\frac{\varepsilon - \varepsilon_0}{2\varepsilon + f_p\varepsilon_0}\boldsymbol{E}_0. \tag{29}$$

The factor f_p is given by Eq. (17) and f_E stands for

$$f_E = \frac{1 + 4\frac{L_Q}{R_{\text{cav}}} + 6\frac{L_Q^2}{R_{\text{cav}}^2} + 6\frac{L_Q^3}{R_{\text{cav}}^3}}{1 + 4\frac{L_Q}{R_{\text{cav}}} + 9\frac{L_Q^2}{R_{\text{cav}}^2} + 9\frac{L_Q^3}{R_{\text{cav}}^3}}. \tag{30}$$

The quadrupolar factor f_E is always smaller than 1. At $L_Q \to 0$, when $f_E = f_p = 1$, Eqs. (26)-(29) simplify to the well-known cavity field for non-quadrupolarizable medium.[14,41] Compared to this classical result, the cavity field in quadrupolarizable medium is always smaller. Unlike the reaction field, the cavity field is affected by the medium's quadrupolarizability even in the case of very polar fluids (because E_{cav} is proportional to f_E). This finding means, by the way, that the interaction between a dissolved dipole and the field of another particle, say, an ion or a second dipole, is affected by L_Q significantly. It is also noteworthy that in the case of purely quadrupolar medium (one of $\varepsilon = \varepsilon_0$), the factor Y_E becomes equal to 1 and the external dipole $\boldsymbol{p}_{\text{ext},E}$ disappears. This means that the external field $\boldsymbol{E}_0$ cannot be distorted by the discontinuity of the quadrupole polarizability alone—only the heterogeneity of ε leads to the distortion. This can be intuitively expected, since quadrupoles do not interact with homogeneous field.

Let us finally solve the problem for a cavity in quadrupolar medium placed in an external electric field gradient $(\nabla\boldsymbol{E})_0$. The solution of Eqs. (5) and (8) for the potential at $r < R_{\text{cav}}$ reads

$$\phi_{\nabla E0} = -\frac{1}{2}\boldsymbol{r}\cdot(\nabla\boldsymbol{E})_{\text{cav}}\cdot\boldsymbol{r}, \tag{31}$$

and the potential outside the cavity is

$$\begin{aligned} \phi_{\nabla E} = &-\frac{1}{2}\boldsymbol{r}\cdot(\nabla\boldsymbol{E})_0\cdot\boldsymbol{r} + \frac{3\boldsymbol{r}\cdot\mathbf{q}_{\text{ext},\nabla E}\cdot\boldsymbol{r}}{8\pi\varepsilon r^5} \\ &\times\left(1 - 15g_q\frac{3\varepsilon - 2\varepsilon_0}{\varepsilon - g_{\nabla E}\varepsilon_0}\frac{r^2 + 3L_Qr + 3L_Q^2}{2R_{\text{cav}}^2}\mathrm{e}^{-\frac{r-R_{\text{cav}}}{L_Q}}\right). \end{aligned} \tag{32}$$

Here, the cavity field gradient $(\nabla\boldsymbol{E})_{\text{cav}}$ is proportional to $(\nabla\boldsymbol{E})_0$,

$$(\nabla\boldsymbol{E})_{\text{cav}} = Y_{\nabla E}(\nabla\boldsymbol{E})_0, \quad Y_{\nabla E} = \frac{5\varepsilon f_{\nabla E}}{3\varepsilon + 2\varepsilon_0 f_q}. \tag{33}$$

The excess quadrupole moment $\mathbf{q}_{\text{ext},\nabla E}$ of the sphere induced by the external gradient $(\nabla \boldsymbol{E})_0$ is given by the equation

$$\mathbf{q}_{\text{ext},\nabla E} = -\frac{8}{3}\pi\varepsilon R_{\text{cav}}^5 \frac{\varepsilon - g_{\nabla E}\varepsilon_0}{3\varepsilon + 2f_q\varepsilon_0}(\nabla \boldsymbol{E})_0. \tag{34}$$

The two quadrupolar factors $f_{\nabla E}$ and $g_{\nabla E}$ stand for the expressions

$$\begin{aligned} f_{\nabla E} &= \frac{1 + 6\frac{L_Q}{R_{\text{cav}}} + 15\left(\frac{L_Q}{R_{\text{cav}}}\right)^2 + 27\left(\frac{L_Q}{R_{\text{cav}}}\right)^3 + 27\left(\frac{L_Q}{R_{\text{cav}}}\right)^4}{1 + 6\frac{L_Q}{R_{\text{cav}}} + 24\left(\frac{L_Q}{R_{\text{cav}}}\right)^2 + 54\left(\frac{L_Q}{R_{\text{cav}}}\right)^3 + 54\left(\frac{L_Q}{R_{\text{cav}}}\right)^4}, \\ g_{\nabla E} &= \frac{1 + 6\frac{L_Q}{R_{\text{cav}}} + 21\left(\frac{L_Q}{R_{\text{cav}}}\right)^2 + 45\left(\frac{L_Q}{R_{\text{cav}}}\right)^3 + 45\left(\frac{L_Q}{R_{\text{cav}}}\right)^4}{1 + 6\frac{L_Q}{R_{\text{cav}}} + 24\left(\frac{L_Q}{R_{\text{cav}}}\right)^2 + 54\left(\frac{L_Q}{R_{\text{cav}}}\right)^3 + 54\left(\frac{L_Q}{R_{\text{cav}}}\right)^4}. \end{aligned} \tag{35}$$

The results (33)-(35) for *quadrupolarized* cavity are analogous to Eqs. (28)-(30) for polarized cavity. As with the cavity field, the cavity field gradient is significantly affected by the quadrupoles in the medium, as $(\nabla \boldsymbol{E})_{\text{cav}}$ is proportional to the quadrupolar factor $f_{\nabla E}$.

In what follows, the results for $\boldsymbol{E}_{\text{react}}$, $\boldsymbol{E}_{\text{cav}}$, $(\nabla \boldsymbol{E})_{\text{react}}$, and $(\nabla \boldsymbol{E})_{\text{cav}}$ will be used to extend Onsager's theory to quadrupolar liquids and to analyze the measurements of the dielectric permittivity of various liquids within this extended theory in order to extract from them the cavity radii and the quadrupolar lengths in these liquids. However, the four results have a much wider field of application—the reaction field and gradient are in the base of the theory of solvation[15–25] and the cavity field and gradient are important for the description of the electrostatic interaction between dissolved particles (and consequently of their activity coefficients, association constants, etc.). These questions will be considered in the future.

C. Local field and local field gradient

Following Onsager,[14] we assume that each molecule in a polarized liquid is subject to a local field $\boldsymbol{E}_{\text{loc}}$ that is the sum of the reaction field (15) and the cavity field (28),

$$\boldsymbol{E}_{\text{loc}} = \boldsymbol{E}_{\text{react}} + \boldsymbol{E}_{\text{cav}} = X_p\boldsymbol{p} + Y_E\boldsymbol{E}_0. \tag{36}$$

The molecule is polarizable (of molecular polarizability α_p). The local field induces a dipole moment $\alpha_p\boldsymbol{E}_{\text{loc}}$ in the central molecule; thus, the total dipole $\boldsymbol{p}$ that the molecule acquires is

$$\boldsymbol{p} = \boldsymbol{p}_0 + \alpha_p\boldsymbol{E}_{\text{loc}}, \tag{37}$$

where $\boldsymbol{p}_0$ is the permanent molecular dipole moment. Here, α_p must be understood as the mean polarizability of the molecules, $\alpha_p = \Sigma\alpha_{p,ii}/3$, where $\alpha_{p,ii}$ are the components of the polarizability tensor. The two vector equations (36) and (37) are solved for $\boldsymbol{p}$ and $\boldsymbol{E}_{\text{loc}}$,

$$\boldsymbol{p} = \frac{\boldsymbol{p}_0 + \alpha_p Y_E\boldsymbol{E}_0}{1 - \alpha_p X_p}, \tag{38}$$

$$\boldsymbol{E}_{\text{loc}} = \frac{X_p\boldsymbol{p}_0 + Y_E\boldsymbol{E}_0}{1 - \alpha_p X_p}. \tag{39}$$

The local field has a component proportional to $\boldsymbol{p}_0$ and a component proportional to the external field—the same is valid for non-quadrupolar media.[14] However, our coefficients X_p and Y_E, Eqs. (15) and (28), are functions of the quadrupolar length L_Q of the medium through the factors f_p and f_E, Eqs. (17) and (30).

Analogously, the local electric field gradient $(\nabla \boldsymbol{E})_{\text{loc}}$ acting on a molecule in quadrupolar medium is the sum of the reaction and the cavity field gradients (28) and (33),

$$(\nabla \boldsymbol{E})_{\text{loc}} = (\nabla \boldsymbol{E})_{\text{react}} + (\nabla \boldsymbol{E})_{\text{cav}} = X_q\mathbf{q} + Y_{\nabla E}(\nabla \boldsymbol{E})_0. \tag{40}$$

Each molecule is *quadrupolarized* by the local field gradient to acquire a total quadrupole moment of

$$\mathbf{q} = \mathbf{q}_0 + \alpha_q\left[(\nabla \boldsymbol{E})_{\text{loc}} - \mathbf{U}(\nabla \cdot \boldsymbol{E})_{\text{loc}}/3\right]. \tag{41}$$

Here, α_q is the mean molecular quadrupolarizability (its relation to the components of the tensor of the molecular quadrupolarizability is derived in Section C of the supplementary material[93]). The term $\mathbf{U}(\nabla \cdot \boldsymbol{E})_{\text{loc}}/3$ is added so that the induced quadrupole has zero trace explicitly; as far as $(\nabla \cdot \boldsymbol{E})_{\text{loc}} = 0$, this is a question of convenience and the term will be skipped below. The tensor equations (40) and (41) are solved for $\mathbf{q}$ and $(\nabla \boldsymbol{E})_{\text{loc}}$,

$$\mathbf{q} = \frac{\mathbf{q}_0 + \alpha_q Y_{\nabla E}(\nabla \boldsymbol{E})_0}{1 - \alpha_q X_q}, \tag{42}$$

$$(\nabla \boldsymbol{E})_{\text{loc}} = \frac{X_q\mathbf{q}_0 + Y_{\nabla E}(\nabla \boldsymbol{E})_0}{1 - \alpha_q X_q}. \tag{43}$$

These equations are analogous to Eqs. (38) and (39) for $\boldsymbol{p}$ and $\boldsymbol{E}_{\text{loc}}$.

According to Eq. (38), the dipole moment of a molecule increases when this molecule is dissolved: $\boldsymbol{p} = \boldsymbol{p}_0/(1 - \alpha_p X_p)$ in the absence of external field. On the other hand, from Eq. (15), it follows that X_p increases with the quadrupole polarizability of the medium, and therefore, the factor $\boldsymbol{p}/\boldsymbol{p}_0$ is larger when quadrupoles are present in the solvent. In addition, the quadrupole moment of the molecule also increases—from Eq. (42), $\mathbf{q} = \mathbf{q}_0/(1 - \alpha_q X_q)$ in the absence of an external field gradient. Indeed, the quadrupole moment of the water molecule is ∼13% higher in the condensed phase compared to gas.[42]

D. Macroscopic polarizability and quadrupolarizability of a quadrupolar insulator

Let the outer field $\boldsymbol{E}_0$ be created by a charge e_∞ at infinite distance from the cavity, with vector-position $\boldsymbol{r}_\infty = (0, 0, -r_\infty)$ (Cartesian coordinates, z-axis in direction of $\boldsymbol{E}_0$). The magnitude of this charge is

$$e_\infty = 4\pi\varepsilon r_\infty^2 E_0. \tag{44}$$

This charge interacts with the total field created by the dipole and the polarized cavity, which is found as the sum of ϕ_p and ϕ_E, Eqs. (14) and (27), at $r \to \infty$,

$$\phi_p + \phi_E\big|_\infty = \frac{(\boldsymbol{p}_{\text{ext}} + \boldsymbol{p}_{\text{ext},E}) \cdot \boldsymbol{r}_\infty}{4\pi\varepsilon r_\infty^3}. \tag{45}$$

The respective interaction energy follows from Eqs. (16), (29), and (38),

$$u_p = \left(\phi_p + \phi_E\right)_\infty e_\infty = -\left(\boldsymbol{p}_{\text{ext}} + \boldsymbol{p}_{\text{ext},E}\right)\cdot \boldsymbol{E}_0 = -\frac{3\varepsilon}{2\varepsilon + f_p\varepsilon_0}\frac{p_0 E_0 \cos\theta}{1-\alpha_p X_p} + O(E_0^2), \tag{46}$$

where θ is the angle between $\boldsymbol{p}_0$ and $\boldsymbol{E}_0$; the terms of $O(E_0^2)$ are neglected. The Boltzmann distribution of θ corresponding to energy (46) is also linearized for small external fields,

$$\rho_p = C_n \exp(-u_p/k_BT) \approx C_n(1 - u_p/k_BT), \tag{47}$$

where the value of the normalizing constant $C_n = 1/2$ follows from the normalization of ρ_p. Note that the cavity field term $\boldsymbol{p}_{\text{ext},E}\cdot \boldsymbol{E}_0$ in Eq. (46) is $O(E_0^2)$ and does not contribute to the linear dielectric response of the medium; $\boldsymbol{p}_{\text{ext},E}\cdot \boldsymbol{E}_0$ is important for the macroscopic hyperpolarizabilities only. The fact that there is no contribution in Eqs. (46) and (47) from the cavity field means that the cavity factor Y_E has no effect on the orientation component of the macroscopic polarizability. The cavity field affects the induced dipole contribution to ε only.

We now take the average of Eq. (38). The average vector $\boldsymbol{p}$ is parallel to $\boldsymbol{E}_0$; if the angle between $\boldsymbol{p}_0$ and $\boldsymbol{E}_0$ is θ, we can write

$$\bar{p} = \frac{p_0}{1-\alpha_p X_p}\overline{\cos\theta} + \frac{\alpha_p Y_E}{1-\alpha_p X_p}E_0. \tag{48}$$

The average $\cos\theta$ is obtained as $\int_{-1}^{1}\rho_p \cos\theta \mathrm{d}\cos\theta$ using the Boltzmann distribution (46), which yields

$$\bar{p} = \frac{Y_E}{1-\alpha_p X_p}\left[\alpha_p + \frac{1}{f_E\left(1-\alpha_p X_p\right)}\frac{p_0^2}{3k_BT}\right]E_0. \tag{49}$$

Multiplying this equation by the concentration C of particles in the liquid, we obtain the linear relation $C\bar{p} \equiv P = \alpha_P E_0$, where the macroscopic polarizability stands for the expression,

$$\alpha_P \equiv \varepsilon - \varepsilon_0 = \frac{Y_E}{1-\alpha_p X_p}\left[\alpha_p + \frac{1}{f_E\left(1-\alpha_p X_p\right)}\frac{p_0^2}{3k_BT}\right]C. \tag{50}$$

This is the sought generalization of Onsager's formula for ε to quadrupolar media.

To give a qualitative idea for the effect of the medium's quadrupolarizability on its polarizability, let us consider two limiting cases. The first one is a solvent made of molecules with negligible polarizability ($\alpha_p = 0$)—in this case, Eqs. (50) and (28) yield

$$\varepsilon - \varepsilon_0 = \frac{3\varepsilon}{2\varepsilon + f_p\varepsilon_0}\frac{p_0^2}{3k_BT}C. \tag{51}$$

For a dipolar liquid, typically it is valid that $\varepsilon \gg \varepsilon_0$ and therefore, the term $f_p\varepsilon_0$ in this equation (stemming from the reaction field) is negligible, with or without quadrupoles. As a result, the dielectric permittivity of a "permanent dipole liquid" is only weakly affected by L_Q. The second limiting case is a medium made of molecules of zero $\boldsymbol{p}_0$,

$$\varepsilon - \varepsilon_0 = \frac{1}{1-\alpha_p X_p}\frac{3f_E\varepsilon}{2\varepsilon + f_p\varepsilon_0}\alpha_p C. \tag{52}$$

In this case, the polarizability $\alpha_P = \varepsilon - \varepsilon_0$ is proportional to the quadrupolar factor f_E (stemming from the cavity field) and in result, the quadrupoles interfere with the dielectric properties of such fluid much more strongly. The fact that the quadrupoles affect the induced dipole (α_p) but not the orientational ($\boldsymbol{p}_0$) component of α_P is related to the cavity field, which contributes to the former term only.

The contribution of the quadrupoles in a medium to the dielectric constant was discussed previously by Patey *et al.*,[32] who found that Kirkwood's correlation factor[43] depends on the molecular quadrupole moment, which roughly corresponds to stating that R_{cav} is a function of L_Q in Onsager's model. Patey *et al.*[32] neglected, however, the direct effect of L_Q on the reaction/cavity fields discussed here.

The respective average quadrupole moment is derived in a similar manner in Section B of the supplementary material.[93] The averaging yields our constitutive relation (4), with the following quadrupole polarizability coefficient:

$$\alpha_Q \equiv 3\varepsilon L_Q^2 = \frac{Y_{\nabla E}}{1-\alpha_q X_q}\left[\alpha_q + \frac{1}{f_{\nabla E}\left(1-\alpha_q X_q\right)}\frac{\mathbf{q}_0{:}\mathbf{q}_0}{10k_BT}\right]C. \tag{53}$$

Of course, in the infinite dilution limit (where $\varepsilon \to \varepsilon_0$, $L_Q \to 0$ and therefore $X_q = 0$ and $Y_{\nabla E} = f_{\nabla E} = 1$), the ideal gas formula (1) is restored. Let us also mention that initially we *postulated* the linear constitutive relation (4) between $\mathbf{Q}$ and $\nabla\boldsymbol{E}$, which was rigorously derived before[9] for ideal gas only. The derivation in Section B of the supplementary material[93] proves the validity of Eq. (4) also for a dense Onsager fluid.

The two Equations (50) and (53), together with the formulae (15), (17), (22), (24), (28), (30), (33), and (35) for the electrostatic X, Y, f, and g factors, set the basic theory of linear isotropic quadrupolar dielectrics.

III. DIELECTRIC CONSTANT

A. The cavity size and the Curie point

The model of Onsager contains one effective parameter—the cavity radius R_{cav}—which is not rigorously defined. Onsager assumed that the following relation holds between the cavity size and density:

$$\frac{4}{3}\pi R_{\text{cav}}^3 = \frac{1}{C}, \tag{54}$$

commenting that[13,44] "*the assumption that the molecules fill the whole volume of the liquid is a makeshift*" and that "*the development of the theory…will involve careful consideration of molecular arrangements, and probably some arbitrary exercise of judgment.*" Assumption (54) is, indeed, arbitrary in the following two respects:

(i) The cavity size R_{cav}, in the sense of an effective parameter of the average distance between the interacting central molecule and solvent molecules in dense fluids, is at best of the same order of magnitude as the one following from the partial molar volume and Eq. (54). At the same time, if the density is high, Eqs. (50)-(53) are sensitive to this

parameter, and 0.1 Å difference in R_{cav} may drastically change the value of ε.

(ii) Eq. (54) sets not only a value of R_{cav} but also fixes its dependence on temperature T and pressure p. The assumption that the coefficient of mechanical compressibility of the cavity is equal to that of liquid water is not confirmed by the experimental data for the partial molar volume of ions[9]—the volume of a cavity was found to depend on pressure much more weakly than water's molar volume, i.e., for all ions, it was found that $1/R_{cav}^{-3} \times \partial R_{cav}^{-3}/\partial p \ll 1/C \times \partial C/\partial p$, in contrast to what follows from Eq. (54). The negligible compressibility of the cavities of dissolved ions is a well-established fact and has been a common approximation for many years.[45,46]

It is therefore not surprising that many other routes and rules for the determination of R_{cav} has been proposed (short review is present in Refs. 17 and 47). Linder and Hoernschemeyer[50] related R_{cav} to the radial distribution function of the fluid. Luo *et al.*[48,49] imposed a condition for equivalency of Onsager's model and the self-consistent reaction field theory to determine R_{cav}. Zhan and Chipman proposed the cavity boundary to be determined by an electronic isodensity surface of the solute.[47] The comparison of our results with the perturbation theory (cf. Eqs. (12) and (18) and the comments thereafter) suggests that $R_{cav} = (\sigma + \sigma_0)/2$ is an appropriate choice in theory, where σ and σ_0 are sizes of the solute and the solvent in the model of Milischuk and Matyushov.[30] Although these methods have advantages over Eq. (54), they are either somewhat arbitrary or too approximate to be applicable for real liquids. To avoid the difficulties arising from this question, we will attack the reverse problem, which is more appropriate for the aims of our paper: we will determine the cavity radius R_{cav} from the measured value of the dielectric constant, as done by Böttcher[51] (thus correcting his radii for the effect of the quadrupoles). Our Eqs. (50) and (53) allow L_Q to be calculated simultaneously. We will show that this approach leads to consistent results for the dependence of R_{cav} on T and p if the quadrupolarizability of the medium is accounted for, and consistent results for L_Q itself, as well. The calculated values of R_{cav} can be used as a useful benchmark for all theories that require this quantity (the reader is referred to Refs. 17 and 47 for many examples and a critical discussion).

Curie point. A feature of the theory of Onsager that he accentuated is that it does not have a permanent dipole-related Curie temperature.[14] This is in contrast with the earlier theory of Debye[52] whose result suggests that at low temperature, an infinite ε (i.e., pyroelectricity/permanent electric polarization) can be expected, in disagreement with the observations. Onsager, however, have not commented on the fact that Eq. (50) still has an unphysical singularity at certain high concentration at which $1 - \alpha_p X_p = 0$ (the factor X_p is proportional to the concentration through $1/R_{cav}^3$, at least according to Eq. (54)). It can be shown from Eqs. (15) and (50) that the liquid reaches a "Curie concentration" when

$$R_{cav}^3 = \alpha_p/4\pi\varepsilon_0. \tag{55}$$

Such a polarizability-related autopolarization is also in contradiction with the observations. This means that Eq. (50) is inapplicable for $R_{cav}^3 < \alpha_p/4\pi\varepsilon_0$ (and also in the vicinity of $R_{cav}^3 = \alpha_p/4\pi\varepsilon_0$). Our result for α_Q of a quadrupolar Onsager fluid has the same defect—Eqs. (22) and (53) predict autoquadrupolarization (corresponding to $\alpha_Q = \infty$ at $1 - \alpha_q X_q = 0$) at a concentration at which

$$R_{cav}^5 = 3\alpha_q/4\pi\varepsilon_0. \tag{56}$$

The relations (55) and (56) set some limits for the parameters of our model and allow for the simplification of the numerical procedures for solving Eqs. (50) and (53) (these have one physical and several parasitic solutions that violate the above conditions).

B. Dielectric constant, quadrupolarizability and cavity size of various liquids

What follows is the special part of this article, where we use our theory to predict the quadrupolar length L_Q and the cavity radius R_{cav} of several liquids as a function of density and temperature. We have analyzed 10 compounds for which theoretical values of the molecular characteristics $\boldsymbol{p}_0$, α_p, $\mathbf{q}_0$, and α_q have been reported in the literature and for which precisely measured values of the dielectric permittivity and density are published. The simplest of them have zero permanent dipole and quadrupole moments (Ar, Kr, Xe, and CH_4); the following four liquids are made of molecules that have non-zero quadrupole moments (N_2, CO_2, CS_2, and C_6H_6), and the final two have both $\boldsymbol{p}_0$ and $\mathbf{q}_0$ different from zero (H_2O and CH_3OH), cf. Table I. Water and methanol are interesting because their quadrupolar lengths have been estimated previously by using the effect of the quadrupolar strength of these solvents on the Born energy of ions and the activity coefficient of dissolved electrolytes.[9,10] In addition, the Stokes shift of coumarin 153 was used[8] to estimate the quadrupolar strengths in carbon dioxide and benzene. The analysis of liquid CH_4, C_6H_6, and CH_3OH is the first step toward modelling the solvent properties of fuel, crude oil, and lubricants. CO_2 and CS_2 are important solvents in practice and are classical examples of quadrupolar liquids. Finally, the liquid Ar, Kr, Xe, and N_2 are interesting for being of rather simple structure and for being studied in great detail at wide range of conditions.

1. Ar

We aim at the determination of the cavity radius R_{cav} and the quadrupolar length L_Q of liquid argon using Eqs. (50) and (53) and accurate measurements of its dielectric permittivity. Data for the static ε have been reported for extreme pressures and low temperatures by several authors.[53–55] Maroulis and Bishop[56] determined theoretically the molecular parameters, α_p and α_q, required in our theory. However, the quadupolarizability affects the dielectric permittivity very weakly (yet measurably) compared to the main effect from α_p. For this reason, a small error in the value of α_p can result in masking the small effect from α_q, and thereafter,

TABLE I. Values of the molecular multipole moments and polarizabilities, and the coefficients in dependence (57) of R_{cav} on ρ.

	Dipole moment p_0 (Cm) $\times 10^{30}$	Polarizability $\alpha_p/4\pi\varepsilon_0$ (Å^3)	Quadrupole moment $(\mathbf{q}_0{:}\mathbf{q}_0)^{1/2}$ (Cm^2) $\times 10^{40}$	Quadrupolarizability $\alpha_q/4\pi\varepsilon_0$ (Å^5)	k_0 (kg/m^3) and k_ρ in Eq. (57)
Ar[a]	0	1.590 1.639[b]	0	0.454	677.2 0.2896
Kr[a]	0	2.488	0	0.913	...
Xe[a]	0	4.105	0	1.936	...
CH_4[a]	0	2.433 2.597[b]	0	1.681	130.48 0.6834
N_2[a]	0	1.737 1.739[b]	4.08	1.12	379.6 0.4952
CO_2[a]	0	2.63 2.98[b]	11.43	2.21	259.5 0.8945
CS_2[a]	0	8.215	8.88	11.40	761.7 0.5254
C_6H_6[a]	0	10.25[c]	24.87	18.42	723.5 0.3022
H_2O[a]	6.204	1.470	8.074 8.073[d]	0.496	Eq. (59)
CH_3OH[a]	6.062 5.638[e]	3.364 3.32[e]	16.436	3.121	1810.0 0.3633

[a]Theoretical values for Ar from Ref. 56; for Kr and Xe from Ref. 59; CH_4 from Ref. 60; N_2 - Ref. 64; CO_2 - Ref. 65; CS_2 - Ref. 70; C_6H_6 - Ref. 7; H_2O - Ref. 79; CH_3OH - Ref. 81.
[b]Experimental value based on data for ε of gaseous Ar, CH_4, N_2, and CO_2, cf. the text.
[c]The average from the experimental values cited in Refs. 74 and 75.
[d]Corrected for the origin coordinates, cf. the text.
[e]These are experimental values cited in Ref. 81.

in unrealistic values of the calculated R_{cav} and L_Q. To avoid that, we take care to evaluate the value of α_p independently, with as high accuracy as possible, from data for ε of the gaseous Ar.

a. Ar (gas). To check the reliability of the theoretical[56] α_p, we compared Onsager's model with the ε and ρ data for gaseous argon. We included in this analysis only the measurements for dilute gas of density $\rho < 80$ kg/m^3—under such conditions, L_Q is unimportant (it leads to difference of less than $10^{-10}\varepsilon_0$ in the predicted ε); in addition, X_p is small since for gas $\varepsilon \approx \varepsilon_0$, Eq. (15), and therefore the term $\alpha_p X_p \ll 1$ can be neglected. In this case, both Onsager's original model and Eq. (50) simplify to the same equation $(\varepsilon{-}\varepsilon_0)(2\varepsilon + \varepsilon_0)/3\varepsilon = \alpha_p C$. We use this simplified formula (which is nearly equivalent to Clausius-Mossotti's[44]) for the exact determination of α_p from the measured ε and C of the gas. We compared the permittivity that follows from $(\varepsilon - \varepsilon_0)(2\varepsilon + \varepsilon_0)/3\varepsilon = \alpha_p C$ with the experimental ones (limited in the range $\rho = 0 - 73$ kg/m^3, $T = 278$-399 K, $p = 4\times10^5$–6×10^6 Pa, $\varepsilon < 1.023\times\varepsilon_0$, 29 experimental points) to find a minimal standard deviation of $dev_\varepsilon = 0.0001\times\varepsilon_0$, close to the experimental accuracy. The analysis of dev_ε as a function of α_p (left as an unknown parameter) reveals that the data agree with the theory when $\alpha_p/4\pi\varepsilon_0$ is 1.639 ± 0.015 Å^3, which means that the value of Maroulis and Bishop[56] (1.590 Å^3) is underestimated (compare also with 1.64 Å^3 in Hill's book[57]). Therefore, we will use the value of α_p that follows from the experimental data for gas when dealing with liquid Ar below. Probably, the theoretical α_q is also lower than the real value, but unlike α_p, an error of several percents in α_q is inessential for the final results for L_Q and R_{cav} of the liquid.

b. Ar (liquid). We now proceed to the liquid argon data from Refs. 53–55. For each measurement of ρ and ε at various p and T, Eqs. (50) and (53) have two unknowns: R_{cav} and L_Q, for which we solve them (for the facilitation of the reader, a sample Maple 18 code for the numerical procedure is provided in Section D of the supplementary material[93]). The results are illustrated in Fig. 3.

Let us first comment on the results for R_{cav}. As seen in Fig. 3(a), the cavity radius varies in a narrow interval, 2.4-2.6 Å, much narrower than Onsager's Eq. (54) would predict. The value of R_{cav} is larger than the hard sphere radius of Ar (1.7 Å) and smaller than the minimal distance between two atoms (3.4 Å)—thus, the relation $R_{cav} = \sigma$ that we expect to hold in the continuum single particle limit of the perturbation theory does not agree with the data for Ar. At low densities, the value of ε is insensitive to R_{cav} and in result the calculated cavity radii become very dispersed. Therefore, we will not discuss the data for $\rho < 750$ kg/m^3 ($C < 19$M). We analyzed the R_{cav} data in Fig. 3(a) to find that

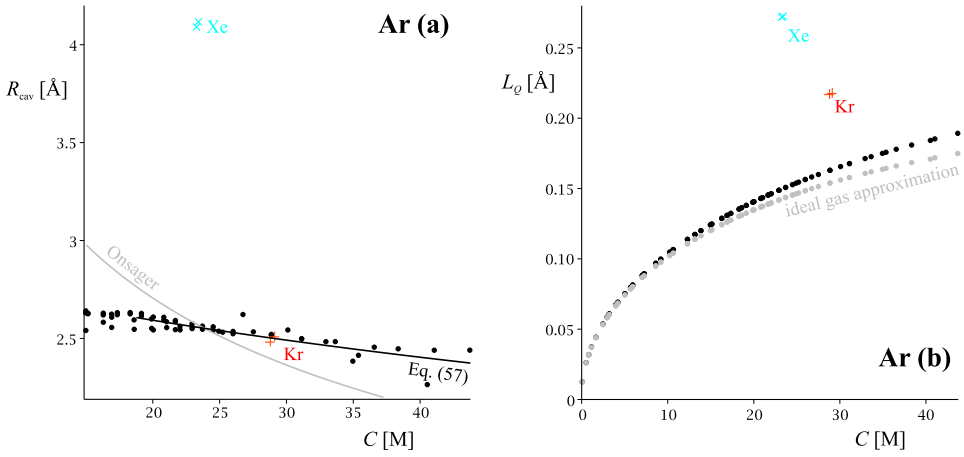

FIG. 3. (a) Cavity radius R_{cav} of liquid argon as a function of molar concentration C, based on data[53–55] for its dielectric permittivity and density and Eqs. (50) and (53). The gray line is R_{cav} according to Onsager's assumption (54). The black line is Eq. (57). Data for Kr and Xe are given for comparison (using ε and ρ by Amey and Cole[55]). (b) Quadrupolar length L_Q as a function of C calculated from the same data and equations. Ideal gas approximation (1) is given for comparison (in gray) for Ar.

$1/R_{cav}^3$ is an almost linear function of ρ and does not depend on the temperature (in the range ρ = 750-1750 kg/m^3, T = 84-399 K, $p = 10^5$-9×10^8 Pa, ε = 1.26-1.65 $\times\,\varepsilon_0$). Therefore, instead of Eq. (54), we tested the following empirical relation:

$$\frac{m}{\frac{4}{3}\pi R_{cav}^3} = k_\rho \rho + k_0; \tag{57}$$

here, m is the atomic mass of Ar. The coefficients k_ρ and k_0 were determined by regression over the experimental data for ε vs. the theoretical permittivity following from Eqs. (50), (53), and (57) (solved for the unknown R_{cav}, L_Q, and ε).[58] The minimization of the respective dispersion of ε yields k_ρ = 0.2896 and k_0 = 677.2 kg/m^3, with standard deviation between the predicted and the experimental permittivities $dev_\varepsilon = 0.0009\times\varepsilon_0$. We can use Eq. (57) to relate the compressibility coefficient of the cavity to the compressibility of the liquid argon,

$$R_{cav}^3 \frac{\partial}{\partial p}\frac{1}{R_{cav}^3} = \frac{\rho}{\rho + k_0/k_\rho}\frac{1}{\rho}\frac{\partial \rho}{\partial p}; \tag{58}$$

a similar relation holds for the coefficients of thermal expansion. From these relations, it follows that the cavity's compressibility and expansion coefficient are lower than $1/\rho\times\partial\rho/\partial p$ and $1/\rho\times\partial\rho/\partial T$ by a factor of $\rho/(\rho + k_0/k_\rho)$ = 0.25-0.4.

The quadrupolar length of Ar is rather small—less than 0.2 Å, Fig. 3(b). For this reason, L_Q can be, in fact, safely neglected in Eq. (50), in which case it simplifies to Onsager's original equation. If, instead of Eq. (50), R_{cav} is calculated from the latter (as Böttcher[51] did), the obtained radii remain almost unchanged. As we will see below, this is not the case with quadrupolar liquids.

In Fig. 3(b), we compare what follows from our Eq. (53) for L_Q with the ideal gas formula (1) (in $L_Q^2 = \alpha_Q/3\varepsilon$, we use the experimental values of ε). As seen, the quadrupolar length of the Onsager fluid does not differ much from the gaseous approximation; the exact quadrupolar length is larger by at most 8%, mostly due to the cavity field gradient factor $Y_{\nabla E}$ in Eq. (53) (while the reaction field gradient term $\alpha_q X_q$ is small).

2. Kr and Xe

The data for ε and ρ of Amey and Cole[55] for liquid Kr and Xe at low temperatures are processed in a similar manner and the results for R_{cav} and L_Q are shown in Fig. 3. The values of Maroulis[59] are used for α_p and α_q (Table I). The calculated cavity radii are quite uncertain for both gases because a tiny error in the values of ε or α_p can lead to significant change of the calculated value of R_{cav}. For example, if instead of[59] $\alpha_p/4\pi\varepsilon_0$ = 4.105 Å^3 the value 4.0 Å^3 of Hill[57] is used for Xe, the calculated R_{cav} will be 3.2 Å instead of 4.1 Å. On the other hand, we found that the values of L_Q are not so sensitive to small errors in the value of ε or α_p and are therefore more trustworthy. According to Fig. 3(b), at a given concentration, the quadrupolar length of the noble gases increases with their atomic number.

3. CH_4

Maroulis[60] calculated the molecular polarizability and quadrupole polarizability of methane ($\boldsymbol{p}_0$ and $\boldsymbol{\mathsf{q}}_0$ are zero). Data for ε and ρ of methane at high pressures have been reported in Refs. 61 and 62.

a. CH_4 (gas). As with the argon, the theoretical value of the polarizability is not accurate enough for our purposes. Therefore, we used the approach for Ar above to extract a very accurate value of α_p from the ε data for gaseous methane. The range of the 36 experimental points used for this is such that $(\varepsilon-\varepsilon_0)(2\varepsilon+\varepsilon_0)/3\varepsilon = \alpha_p C$ holds: ρ < 40 kg/m^3, T = 125-600 K, $\varepsilon < 1.048\times\varepsilon_0$, $p = 10^5$-10^7 Pa. The polarizability found from these data is $\alpha_p/4\pi\varepsilon_0 = 2.597\pm0.003$ Å^3, with $dev_\varepsilon = 0.000\,02\times\varepsilon_0$, approaching the experimental accuracy. This result compares well with 2.59 Å^3 in Ref. 57 but is significantly higher than the theoretical value[60] 2.4 Å^3.

b. CH_4 (liquid). The measured[61,62] ε and ρ of dense CH_4 have been dealt with in the same way as those for liquid Ar to determine methane's cavity radius and quadrupolar length (data range: ρ up to 455 kg/m^3, T = 90-300 K, $p = 10^5$-3.5×10^7 Pa, ε up to $1.68\times\varepsilon_0$; we used the experimental α_p and the theoretical α_q from Table I). The values of R_{cav} and L_Q calculated from Eqs. (50) and (53) are illustrated in Fig. 4 as functions of ρ.

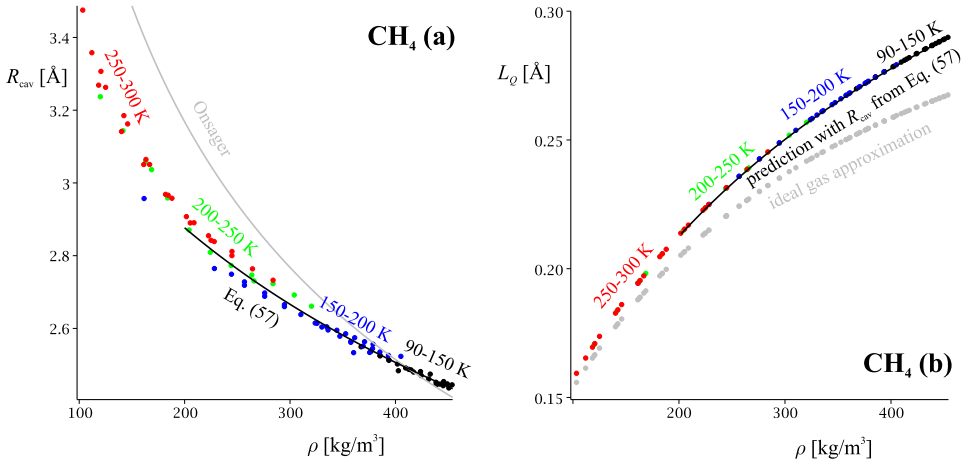

FIG. 4. (a) The cavity radius of dense methane as a function of ρ at several temperatures (based on data from Refs. 61 and 62 and Eqs. (50) and (53)). The colour indicates the temperature. The gray line is Onsager's assumption Eq. (54), the black one—Eq. (57) ($k_\rho = 0.68$ and $k_0 = 130$ kg/m^3). (b) Quadrupolar length L_Q of dense methane, calculated from the same data. Gray dots: Eqs. (1) and (6); black line is the theoretical prediction using (50), (53), and (57).

R_{cav} decreases from 3.5 to 2.5 Å (compare to the van der Waals radius of CH_4, 2 Å). The determined R_{cav} are nearly equal to those following from Böttcher's approach (i.e., from Eq. (50) with $L_Q = 0$; not shown) and are significantly lower than Onsager's assumption (54). The data points fall approximately on a single curve, which suggests that R_{cav} is a function of the density only (note the wide temperature interval). The analysis of the curve shows that Eq. (57) holds within the dispersion of the calculated R_{cav}. To determine the coefficients k_ρ and k_0 in Eq. (57), we used only the data with $\rho > 200$ kg/m^3 where the data points are less dispersed. The minimization of the dispersion of the theoretical permittivity following from Eqs. (50), (53), and (57) vs. the experimental ε yields $k_\rho = 0.6834$ and $k_0 = 130.48$ kg/m^3, with standard deviation $dev_\varepsilon = 0.0004 \times \varepsilon_0$.

The quadrupolar length in Fig. 4(b) increases with ρ from 0.15 to 0.3 Å. At a given density, L_Q is independent of the temperature within the dispersion of the calculated values (according to Eq. (53); this is possible only because R_{cav} is independent of T). As with argon, the exact L_Q is slightly higher than the one following from ideal gas formula (1) and Eq. (6).

4. N_2

The liquid nitrogen is our first example of a true quadrupolar liquid since it has non-zero permanent quadrupole moment $\mathbf{q}_0$ and zero permanent dipole moment $\boldsymbol{p}_0$. Accurate data for the dielectric permittivity and density are available[61,63] for gaseous and liquid nitrogen. Maroulis and Thakkar[64] used fourth order many-body perturbation theory to calculate the required molecular characteristics (α_p, α_q, and $\mathbf{q}_0$) of N_2.

a. N_2 (gas). We checked the reliability of the theoretical[64] α_p by using the equation $(\varepsilon - \varepsilon_0)(2\varepsilon + \varepsilon_0)/3\varepsilon = \alpha_p C$ to determine α_p from the data for gaseous nitrogen (we analyzed only the measurements for densities $\rho < 100$ kg/m^3, where the quadrupole terms and the value of R_{cav} are unimportant for the predicted ε). The permittivity that follows from this equation is compared with the experimental ε in the range ρ = 0-100 kg/m^3, T = 77-1500 K, $p = 10^5$-10^7 Pa, $\varepsilon < 1.047 \times \varepsilon_0$, 38 data points. The analysis of dev_ε as a function of α_p (left as variable) leads to best value $\alpha_p/4\pi\varepsilon_0 = 1.739 \pm 0.005$ Å^3, which means that the value of Maroulis and Thakkar (1.737 Å^3) is accurate; for comparison, Hill[57] gives 1.74 Å^3. The minimal standard deviation is $dev_\varepsilon = 0.000\,05 \times \varepsilon_0$, close to the experimental accuracy.

b. N_2 (liquid). We analyze the data from Refs. 61 and 63 for liquid nitrogen (in the range ρ up to 870 kg/m^3, T = 63-300 K, $p = 10^5$-3.5×10^7 Pa, ε up to $1.5 \times \varepsilon_0$). The theoretical values are used for α_p, α_q, and $\mathbf{q}_0$ (Table I). For each measured ρ and ε, Eqs. (50) and (53) are solved for the two unknowns: R_{cav} and L_Q. The results are illustrated in Fig. 5.

Let us first consider the magnitude of the effect of L_Q on the value of the dielectric permittivity ε for quadrupolar liquid such as N_2. This effect is stronger for dense fluids, where L_Q is high and R_{cav} is low (so that the quadrupolar f and g factors differ more from 1, cf. Eqs. (17), (24), (30), and (35)). Taking the datum[61] for the densest nitrogen (namely, $\rho = 871.778$ kg/m^3, $\varepsilon = 1.470\,67 \times \varepsilon_0$ at $T = 65.32$ K, $p = 10^7$ Pa), we solve Eqs. (50) and (53) to find that $L_Q = 1.21$ Å and $R_{cav} = 2.39$ Å at this pressure and temperature. If we now use the same cavity radius but neglect L_Q in Eq. (50) (i.e., if we use Onsager's original equation), we can determine from it $\varepsilon = 1.472\,44 \times \varepsilon_0$. Therefore, the direct effect of the quadrupoles on the dielectric permittivity is to decrease it by $1.472\,44$–$1.470\,67 \approx 0.002 \times \varepsilon_0$, due to the decrease of the cavity field in the presence of quadrupoles (decreased Y_E in Eq (50)). This effect is 100 smaller than the main contribution from the polarizability α_p of N_2, yet, it is 100 larger than the experimental precision, so the accurate measurements of the dielectric constant are indeed suitable for the determination of L_Q. It is also interesting to compare the quadrupole moment $\mathbf{q}$ of N_2 in the liquid phase with $\mathbf{q}_0$ in gaseous phase. From Eq. (42), it follows that $\mathbf{q}$ increases by several percents. For the values above for ρ, ε, R_{cav}, and L_Q at $T = 65.32$ K, $p = 10^7$ Pa, we calculate $1/(1 - \alpha_q X_q) = 103.2\%$.

Let us discuss now the quadrupolar length of N_2. For molecules of non-zero $\mathbf{q}_0$, from Eq. (53), it follows that L_Q is a function of temperature as seen in Fig. 5(b). This results also in a weak dependence of ε on T at fixed ρ, which is absent in Onsager's original theory. The outcome is an artificial dependence of Böttcher's R_{cav} on T. This is illustrated in Fig. 5(a): the radii that follow from Eq. (50) with

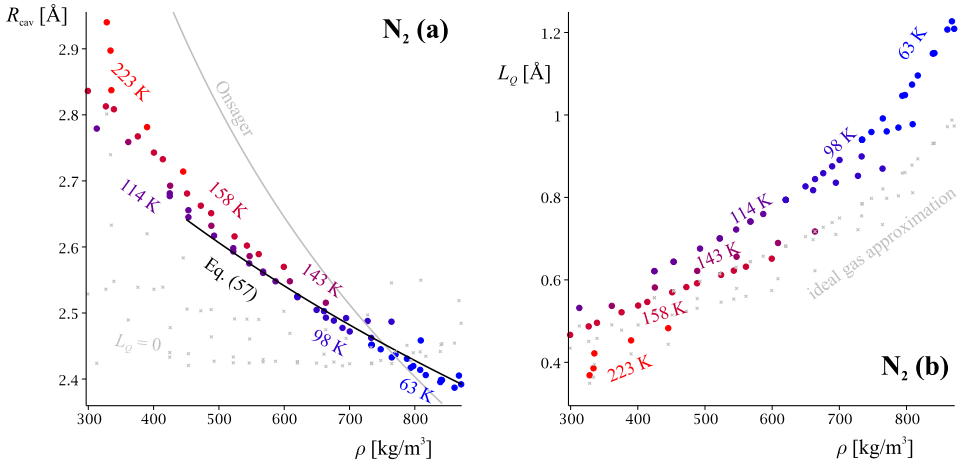

FIG. 5. (a) The cavity radius of N_2 calculated from Eqs. (50) and (53) and experimental data for static ε and ρ from Refs. 61 and 63. The colour indicates the temperature. The gray symbols are Böttcher's R_{cav} following from the original theory of Onsager (Eq. (50) with $L_Q = 0$). The black line is Eq. (57) with $k_\rho = 0.50$ and $k_0 = 380$ kg/m^3. (b) The quadrupolar length L_Q following from the same model and data. Gray dots: ideal gas approximation for α_Q, Eqs. (1) and (6), calculated with the experimental values of ε.

$L_Q = 0$ are highly dispersed and show strong dependence on T. However, when the quadrupolarizability of the medium is accounted for, R_{cav} becomes a neat function of ρ only. Thus, the temperature dependence of nitrogen's ε and Böttcher's R_{cav} turns out to be consequence of the quadrupolar strength of the liquid.

The data in Fig. 5(a) again agree well with linear dependence of $1/R_{cav}^3$ on ρ for densities above 450 kg/m^3 (below that density, ε does not depend strongly on R_{cav} and the calculated radii are uncertain). We tested Eq. (57) by regression analysis of the experimental data for nitrogen's ε vs. the permittivity predicted from our Eqs. (50), (53), and (57) (solved for the unknown R_{cav}, L_Q and ε). The minimization of the respective dispersion yields $k_\rho = 0.4952$ and $k_0 = 379.6$ kg/m^3, with standard deviation between the predicted and the experimental permittivities $dev_\varepsilon = 0.0005 \times \varepsilon_0$. These values and Eq. (58) suggest that the compressibility of the nitrogen's cavity is about twice smaller than the compressibility of the liquid N_2 at $\rho > 450$ kg/m^3.

5. CO_2

a. CO_2 (gas). Unlike the polarizability of N_2, the reported theoretical α_p of CO_2 differ significantly from the experimental ones. Even the highest theoretical value we found[65] is significantly smaller than the one following from measurements of ε of the dilute gas. Using data for gaseous CO_2 from Refs. 66–68, we find as for Ar, CH_4, and N_2 above that for carbon dioxide, $\alpha_p/4\pi\varepsilon_0 = 2.98 \pm 0.02$ Å^3 (leading to $dev_\varepsilon = 0.0002 \times \varepsilon_0$ in the range ρ = 0-75 kg/m^3, T = 273-373 K, $p = 10^6$-4×10^6 Pa, $\varepsilon < 1.039 \times \varepsilon_0$, 22 data points).

b. CO_2 (liquid). We used then the data by Moriyoshi *et al.*[66] and Eqs. (50) and (53) to calculate the radii and the quadrupolar lengths in Fig. 6 (ρ up to 1050 kg/m^3, T = 273-353 K, $p = 10^6$-3×10^7 Pa, ε up to $1.67 \times \varepsilon_0$). For α_q and $\mathbf{q}_0$, we use the theoretical values of Maroulis, α_p is the experimental one (Table I).

As with N_2, for liquid CO_2, there is a significant difference between Böttcher's radii and ours. Onsager's original equation for $\varepsilon(R_{cav})$ leads to artificial dependence of R_{cav} on T while our radii depend on ρ only (within the dispersion of the points). The data in Fig. 6(a) agree with Eq. (57) for R_{cav} vs. ρ. The coefficients k_ρ and k_0 were determined as above, from regression over the experimental data with ε vs. density predicted from Eqs. (50), (53), and (57) (solved for the unknown R_{cav}, L_Q, and ε). The minimization of the dispersion for the data[66] above $\rho > 750$ kg/m^3 yields $k_\rho = 0.8945$ and $k_0 = 259.5$ kg/m^3, with standard deviation

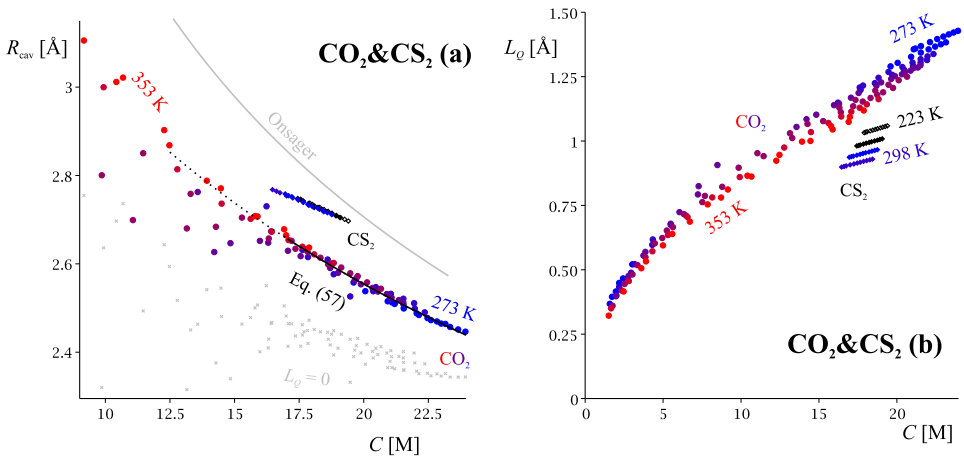

FIG. 6. (a) Cavity radius of CO_2 and CS_2 as a function of their concentration C, calculated with Eqs. (50) and (53) and experimental data[66,69] for ε and ρ. The colour indicates the temperature. The gray symbols are Böttcher's R_{cav} following from Onsager's original equation (Eq. (50) with $L_Q = 0$). Gray line is Eq. (54); black line is Eq. (57) with $k_\rho = 0.89$ and $k_0 = 260$ kg/m^3 for CO_2. (b) The quadrupolar length L_Q following from the same model.

between the predicted and the experimental permittivities $dev_\varepsilon = 0.0009 \times \varepsilon_0$.

The quadrupolar length reaches significant values. For the datum[66] for the densest CO_2 (namely, $T = 273.15$ K, $\rho = 1054.3$ kg/m^3, $p = 30$ MPa, $\varepsilon = 1.670\,92 \times \varepsilon_0$), we find from Eqs. (50) and (53), $R_{cav} = 2.45$ and $L_Q = 1.43$ Å. If Onsager's equation is used instead of Eq. (50) (i.e., if L_Q is set equal to 0), the value $R_{cav} = 2.45$ Å corresponds to a dielectric permittivity of $\varepsilon = 1.663\,74 \times \varepsilon_0$. Thus, the quadrupoles contribute with about $+0.007 \times \varepsilon_0$ to the value of the dielectric constant—an effect in the opposite direction in comparison with N_2, which is due to the increase of the reaction field in the presence of quadrupoles (for the highly polarizable CO_2 molecule, the X_p reaction factor in Eq. (50) is more important than the cavity field factor Y_E). At these conditions, according to Eq. (42), the quadrupole moment $\mathbf{q}$ of the CO_2 in liquid state increases compared to $\mathbf{q}_0$ for gas by a factor of $\mathbf{q}/\mathbf{q}_0 = 1/(1 - \alpha_q X_q) = 1.065$.

Our results can be tentatively compared with the C_Q coefficient that Jeon and Kim[8] determined from the Stokes shift of coumarin 153 in liquid CO_2, which yields $\alpha_Q = 8\pi\varepsilon_0 C_Q/3 = 0.42 \times 10^{-30}$ F m at $\rho = 800$ kg/m^3 (18.2M) and room temperature. Our values of ε, L_Q and α_Q at these conditions are $\varepsilon = 1.48 \times \varepsilon_0$, $L_Q = 1.2$ Å and $\alpha_Q = 3\varepsilon L_Q^2 = 0.58 \times 10^{-30}$ F m (with R_{cav} from Eq. (57) and parameters from Table I).

6. CS_2 (liquid)

Data for ε and ρ of the liquid are taken from Mopsik.[69] The values of α_p, α_q, and $\mathbf{q}_0$ in Table I are due to Maroulis.[70] The calculated R_{cav} for all data points (in the range $\rho = 1255$-1480 kg/m^3, $T = 223$-298 K, $p = 10^5$-2×10^8 Pa, $\varepsilon = 2.6$-$3.1 \times \varepsilon_0$) fall on a single R_{cav} vs. ρ curve, Fig. 6(a), which agrees with Eq. (57). The values $k_\rho = 0.5254$ and $k_0 = 761.7$ kg/m^3 are determined from the comparison of Eqs. (50), (53), and (57) with the experimental ε and ρ. They correspond to $dev_\varepsilon = 0.0018 \times \varepsilon_0$.

The cavity radii of CS_2 are compared to those of CO_2 in Fig. 6(a). The comparison demonstrates clearly that the cavity radius is specific for each molecule, which is contrary to what follows from Onsager's assumption (54) (which predicts the same value of R_{cav} for any gas of concentration C). The CS_2 cavity is larger and less compressible than that of CO_2 of the same concentration. The quadrupolar length of CS_2 is smaller than that of CO_2—although CS_2 has higher α_q and $\mathbf{q}_0$ than CO_2, it also has larger R_{cav} and ε which lead to the decreased L_Q.

CS_2 is notorious with its large molecular quadrupole polarizability α_q—a quantity that has been largely neglected in the literature. However, it is far from negligible: if α_q is neglected, the calculated quadrupolar lengths of CS_2 will be smaller by about 30% (corresponding to α_Q smaller by 50%).

7. C_6H_6 (liquid)

Data for ε and ρ of the liquid are taken from Refs. 71–73 (in the range $\rho = 834$-946 kg/m^3, $T = 297$-337 K, $p = 10^5$-1.6×10^8 Pa, $\varepsilon = 2.2$-$2.4 \times \varepsilon_0$). The values of α_q and $\mathbf{q}_0$ are reconstructed from the scarce notes of Jeon and Kim.[7] For α_p, we use the average of the experimental values cited in Refs. 74 and 75. The values $k_\rho = 0.3022$ and $k_0 = 723.5$ kg/m^3 are determined from the comparison of Eqs. (50), (53), and (57) with the experimental ε and ρ. They correspond to $dev_\varepsilon = 0.0019 \times \varepsilon_0$.

There are several interesting features of the results for benzene. First, it has quadrupolar length larger than L_Q of any other liquid studied here. At room temperature and normal pressure, where[14] $\rho = 874$ kg/m^3 and $\varepsilon = 2.276 \times \varepsilon_0$, our Eqs. (50) and (53) yield $R_{cav} = 3.15$ Å and $L_Q = 2.0$ Å. The respective macroscopic quadrupolarizability is $\alpha_Q = 3\varepsilon L_Q^2 = 2.4 \times 10^{-30}$ F m. At the same time, gas formula (1) gives much lower values ($L_Q = 1.4$ Å and $\alpha_Q = 1.15 \times 10^{-30}$ F m). Jeon and Kim determined α_Q from Stokes shift data of coumarin in C_6H_6 and obtained $\alpha_Q = 8\pi\varepsilon_0 C_Q/3 = 2.6 \times 10^{-30}$ F m. This compares well with our value, but the coincidence might be accidental since the Stokes shift formula of Jeon and Kim is based on a set of boundary conditions different from Eq. (8).

The comparison of our cavity radii in Fig. 7(a) with those stemming from the original theory of Onsager (Eq. (50) with $L_Q = 0$) demonstrates a clear advantage of our model. If the quadrupolar length is neglected, the calculated R_{cav} has unphysical dependence on ρ—the cavity size expands in a

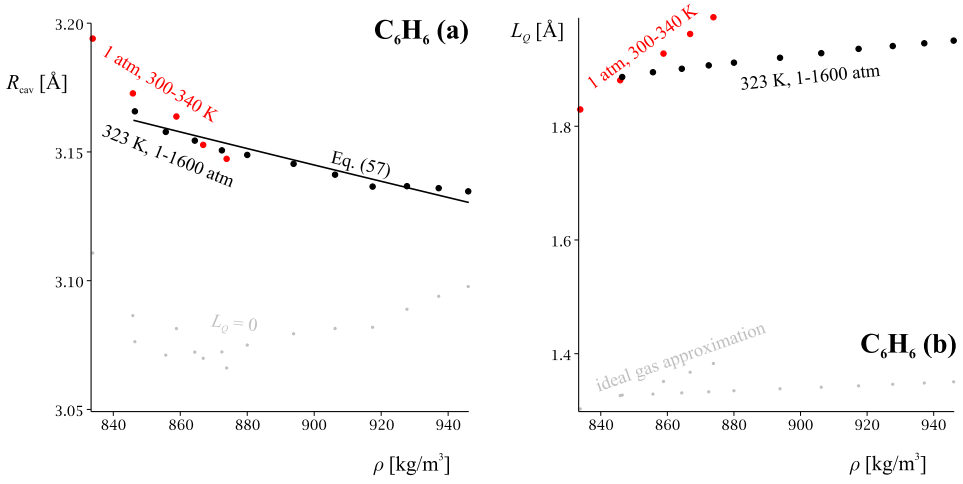

FIG. 7. (a) Cavity radius of C_6H_6 as a function of ρ, calculated with Eqs. (50) and (53) and experimental data for ε and ρ from Refs. 71–73. The red circles[71] correspond to various temperatures and pressure 1 atm, and the black[72]—to various pressures and temperature 323 K. The gray symbols are Böttcher's R_{cav} following from Onsager's equation (Eq. (50) with $L_Q = 0$). The black line is Eq. (57) with $k_\rho = 0.30$ and $k_0 = 720$ kg/m^3. (b) The quadrupolar length L_Q following from the same model. Gray dots: ideal gas approximation for α_Q, Eqs. (1) and (6), with the experimental ε.

denser fluid, which corresponds to negative compressibility (gray dots above 880 kg/m^3). Our values of R_{cav} calculated with the quadrupolar generalization of Onsager's model display normal behaviour. The apparent negative compressibility of Böttcher's radii can be traced to the increase of L_Q with ρ, Fig. 7(b).

8. H_2O (liquid)

Water is by far the best studied fluid—data for the dielectric permittivity[76] and the density[76–78] are available for a wide range of conditions. Yet water is a problematic fluid to study and is interesting as an example for the failure of Onsager's model. The problems start in gas phase, where H_2O has a significant tendency for dimerization, which complicates the direct experimental determination of its permanent dipole and polarizability—for this reason, there is some disagreement in the values of $\boldsymbol{p}_0$ and α_p reported in the literature by different authors. For $\boldsymbol{p}_0$, α_p, $\mathbf{q}_0$, and α_q, we use the theoretical values reported by Batista *et al.*,[79] cf. Table I (these are higher than the theoretical values of Bishop and Pipin[80] and Huiszoon[81] but compare well to the experimental α_p and $\boldsymbol{p}_0$ reported in Refs. 74 and 75). Liquid water, on the other hand, is problematic with its significant conductivity. It leads to a much lower accuracy of the experimental ε (of the order of $0.01 \times \varepsilon_0$). But the largest problem is that a water molecule in liquid phase, with its high dipole moment and small size, creates an extremely large field that leads to nearly complete dielectric saturation in the vicinity of the cavity—this means that Onsager's model (and Eqs. (46) and (47) in particular) is in serious error and leads to spurious results, as we show below.

Note that the value of $\mathbf{q}_0$ of a polar molecule depends on the choice of origin. For the sake of accuracy, we transferred the value of $\mathbf{q}_0$ of Batista *et al.* from his coordinate system (origin in the centre of mass of H_2O) to one with origin in the centre of the O atom, which agrees better with the geometry of Onsager's model. The relation $\mathbf{q}_0 = \mathbf{q}_{0,\text{Batista}} + \boldsymbol{p}_0\Delta\boldsymbol{r} + \Delta\boldsymbol{r}\boldsymbol{p}_0$ was used for this transfer, where $\Delta\boldsymbol{r}$ is the vector-position of the origin of Batista *et al.* in an O-centred coordinate system. The final result for $\mathbf{q}_0$:$\mathbf{q}_0$ is not affected significantly (cf. Table I).

We limited ourselves with the data[76] for liquid water in the range 268-373 K (supercooled water included), up to 3×10^8 Pa, ρ = 960-1100 kg/m^3, ε = 55-90 $\times \varepsilon_0$. The results for R_{cav} and L_Q vs. ρ are shown in Fig. 8. Both are almost constant—in the whole range of conditions, R_{cav} varies in the range 1.40-1.43 Å (perhaps fortuitously, this is very close to water's van der Waals radius), and L_Q varies between 0.28 and 0.29 Å.

Unlike the cases of Ar, CH_4, N_2, and CO_2, there is a small but statistically significant dependence of R_{cav} on temperature. Therefore, instead of Eq. (57), we tested a linear function that involves this temperature dependence,

$$\frac{m}{\frac{4}{3}\pi R_{cav}^3} = k_\rho \rho - k_T T + k_0. \tag{59}$$

We compared the theoretical permittivities that follow from Eqs. (50), (53), and (59) with 183 data points for ε; the dispersion was minimized with respect to the parameters of Eq. (59), leading to best values k_0 = 2765.9 kg/m^3, k_ρ = 0.1264, and k_T = 1.1137 kg/m^{3}K. The minimal standard deviation is $dev_\varepsilon = 0.2 \times \varepsilon_0$.

The value that follows from Eq. (58) for $R_{cav}^3 \partial R_{cav}^{-3}/\partial p$ at room temperature is nearly 20 times lower than water's own compressibility $\rho^{-1}\partial\rho/\partial p$. This is in agreement with the well-established fact that the cavities of ions in water are incompressible.[9] On the other hand, $-R_{cav}^3 \partial R_{cav}^{-3}/\partial T$ and $-\rho^{-1}\partial\rho/\partial T$ are of the same order of magnitude, again in agreement with what was found for ions[9] (though for ions $-R_{cav}^3 \partial R_{cav}^{-3}/\partial T \approx -\rho^{-1}\partial\rho/\partial T$ while at room temperature our $-R_{cav}^3 \partial R_{cav}^{-3}/\partial T$ is about twice larger than $-\rho^{-1}\partial\rho/\partial T$ = 0.000 26 K^{-1}).

The value of L_Q we found here, 0.3 Å, is twice as large as the value following from the gaseous Eq. (1) (which is 0.16 Å at room temperature), yet, it is still by an order of magnitude smaller than our previous estimations—by analyzing data for partial molar volumes, partial molar entropies[9] and activity coefficients[10] of aqueous electrolytes, we estimated L_Q at about 2 Å. This discrepancy indicates that there is a problem with the applicability of the cavity model in linear approximation to aqueous solutions. To demonstrate this, we analyzed the other consequences of Onsager's theory. Let us first calculate the dipole moment of water in the liquid phase. According to Eq. (38) (with $\boldsymbol{E}_0 = 0$), the value of $\boldsymbol{p}$ is larger than $\boldsymbol{p}_0$ by a factor of $1/(1 - \alpha_p X_p)$ = 2.07, due to the extremely high reaction field

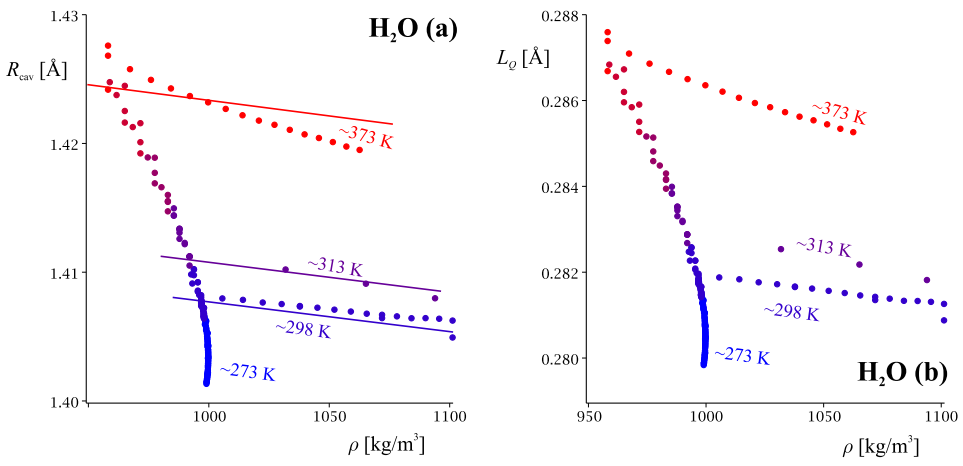

FIG. 8. (a) Cavity radius of H_2O calculated from Eqs. (50) and (53) and experimental data for ε and ρ from Refs. 76–78. The colour indicates the temperature. The lines are Eq. (59) at the indicated temperatures. (b) The quadrupolar length L_Q following from the same model.

($E_{react} = X_p p = 4 \times 10^{10}$ V/m). Although the factor is indeed significant (the increase is 167% in ice[79] and probably around 159% in liquid[82] at normal conditions), 207% is clearly an overestimation. Analogously, according to our model and Eq. (42), the quadrupole moment increases by a factor of $\mathbf{q}/\mathbf{q}_0 = 1/(1 - \alpha_q X_q) = 1.36$. A more probable value of this factor is[42] 1.13.

There are several approximations in Onsager's model that fail in water according to the above numbers. Two of them are the neglected hyperpolarizability and dipole-quadrupole polarizability of the water molecule.[79] Another problem is related to the fact that liquid water is too close to its α_p-related Curie point where we expect Onsager's model to fail—according to Eq. (55), the singularity is at $R_{cav} = 1.14$ Å which is dangerously close to the value 1.4 Å in Fig. 8(a). But the most important failure seems to be the assumed linear equation of state $\boldsymbol{P} = (\varepsilon - \varepsilon_0)\boldsymbol{E}$ of the continuum near the cavity. The field $\boldsymbol{E}$ in the liquid phase can be obtained from Eq. (14); in the range $r = R_{cav} - 3R_{cav}$, using the results for the parameters at room temperature, we obtain that the maximal value of E_r varies in the range 10^{11}-10^{10} V/m. This field is very high and dielectric saturation will inevitably occur in the first layer of water molecules (the first neighbours will be oriented). The neglect of this effect will lead to a significant overestimation of the reaction field which is indeed the case. If one uses $\boldsymbol{P} = (\varepsilon - \varepsilon_0)\boldsymbol{E}$ and the field following from Eq. (14), integration of $\boldsymbol{P}$ in the range $\boldsymbol{r} = R_{cav} - 3R_{cav}$ will result in a dipole moment per each water molecule in the first coordination shell of the order of $50 \times p_0$, while even at complete dielectric saturation, it cannot exceed p_0 (putting aside the molecular polarizability). Therefore the reaction of the medium in the vicinity of the cavity is overestimated by a factor of 50, and this region has a significant contribution to the reaction field. Let us also mention that a saturated layer also goes with fixed quadrupole moment—a sort of *orientational dipole-quadrupole polarizability* stemming from the Boltzmann factor $\exp[-(u_p + u_q)/k_B T]$. This effect is neglected in our study—our assumption that the two components of the Boltzmann distribution (Eq. (46) and Eq. (66) in the supplementary material[93]) can be dealt with separately is valid only for $(u_p + u_q) \ll k_B T$.

We can conclude that a linear Onsager model involving the constitutive relation $\boldsymbol{P} = \alpha_P \boldsymbol{E}$ is inapplicable for water. The same is valid for the Born energy expression used in Refs. 9 and 10 for extracting water's L_Q from experimental data. Therefore, both $L_Q = 0.3$ and 2 Å involve a very significant approximation and are probably correct only within an order of magnitude.

9. CH_3OH (liquid)

Huiszoon[81] calculated the theoretical $\boldsymbol{p}_0$, α_p, $\mathbf{q}_0$, and α_q of methanol given in Table I. Since his results for water are not too accurate, we expected the same to be valid for methanol. We therefore use the experimental values provided in Ref. 81 for $\boldsymbol{p}_0$ and α_p, which agree well also with those by Hill.[57]

Data for the dielectric permittivity and density of liquid CH_3OH from Refs. 83–87 are analyzed. The results for methanol's R_{cav} and L_Q are similar to those obtained for water, Fig. 9. Both R_{cav} and L_Q vary little in the considered range (T = 270-330 K, ρ = 750-860 kg/m^3, p up to 1.1×10^8 Pa, $\varepsilon = 26\text{-}38 \times \varepsilon_0$). R_{cav} is close to 1.83 ± 0.1 Å, which is slightly higher than Böttcher's cavity radius. The quadrupole length varies in the range 0.8-0.81 Å and is 2.4 times larger than the one following from the gaseous equation (1). It compares satisfactorily with the quadrupolar length of methanol obtained from the data for the activity coefficient of NaBr in methanol solution,[10] $L_Q = 1.1 \pm 0.2$ Å.

The difference between the theoretical value 0.81 Å and the experimental one, $L_Q = 1.1 \pm 0.2$ Å, is probably due to the problems we found with water. Methanol's cavity size, 1.82 Å, is relatively close to the quadrupolar Curie point (56) (1.56 Å), where our model is expected to fail. According to Eq. (38), the dipole moment $\boldsymbol{p}$ of methanol is higher than $\boldsymbol{p}_0$ by a factor of 2.16, which is too high, and reaction field (15) is of magnitude 2×10^{10} V/m which is large enough for hyperpolarizability to play a role. The field in the vicinity of the cavity that follows from Eq. (14) varies between 0.3 and 4×10^{10} V/m in the range $r = R_{cav} - 3R_{cav}$. This is much smaller than the field around a cavity in water, which explains the reasonable value we obtained for L_Q. Yet saturation effect must be significant also for methanol. Another problem with methanol is that its molecule is not spherical. The cavity radius

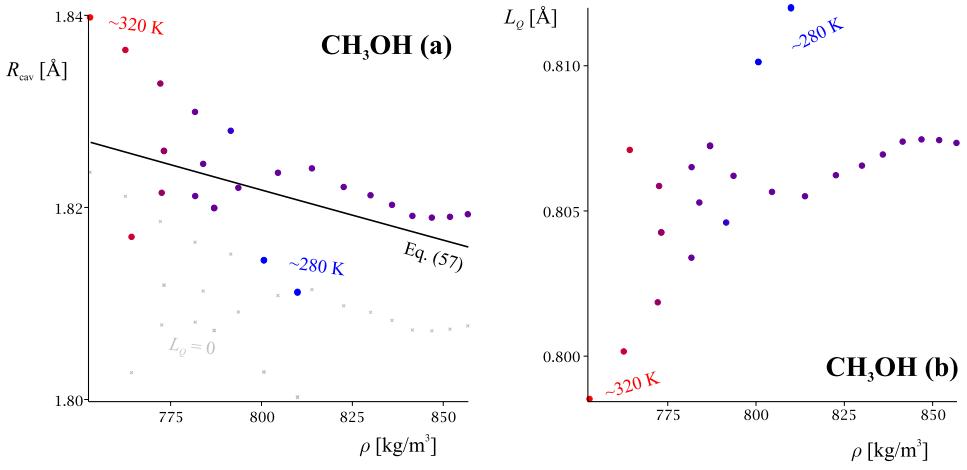

FIG. 9. (a) The cavity radius of CH_3OH calculated from Eqs. (50) and (53) and experimental data for static permittivity and density from Refs. 83–87. The colour indicates the temperature. The black line is Eq. (57). The gray symbols are Böttcher's radii (obtained from Eq. (50) with $L_Q = 0$). (b) The quadrupolar length L_Q following from the same model.

we obtained (1.83 Å) is smaller than the van der Waals radius of the $-CH_3$ group alone. Since R_{cav} that we calculate is an effective characteristic of the polar properties of the liquid (as far as we calculate it from ε), it is not surprising that the size of the small and polar –OH group (1.4 Å) seems to control the value of R_{cav}.

The data in Fig. 9(a) agree within the dispersion of the data points with Eq. (57). We determined the coefficients $k_\rho = 0.3633$ and $k_0 = 1810.0\ kg/m^3$ as above; the deviation of our theory against the experimental data for ε corresponding to these values is $dev_\varepsilon = 0.7 \times \varepsilon_0$, close to the deviation between the measurements of different authors (liquid methanol has significant conductivity which complicates the measurement of ε).

IV. DISCUSSION

The most important theoretical results of this paper are the following:

(i) The reaction field and reaction field gradient have been calculated for quadrupolar medium, Eqs. (15) and (22). These expressions can be used for the analysis of a large family of problems, such as those for the electrostatic contribution from the (non-polar) solvent-(polar) solute interaction to the chemical potential of dissolved species, to the solvatochromic effect, to the kinetic rate constants in solution, etc.

(ii) The cavity field and field gradient have also been calculated, Eqs. (28) and (33). They stand in the base of another family of problems for the electrostatic interactions between charged and polar particles through non-polar medium, and can be used for the calculation of the respective virial coefficients and association constants in solution.

In Sec. II D, the results for $\boldsymbol{E}_{react}$, $\boldsymbol{E}_{cav}$, $(\nabla \boldsymbol{E})_{react}$, and $(\nabla \boldsymbol{E})_{cav}$ have been used to generalize the classical spherical cavity model of Onsager[14] to a linear fluid dielectric made of molecules of non-zero quadrupole moment $\mathbf{q}_0$ and quadrupole polarizability α_q. Like the original model, our generalization allows the calculation of the dielectric permittivity of the fluid provided that the cavity size is known. What is new is that our model also gives the macroscopic quadrupolarizability α_Q of the solvent. We applied it to 10 fluids of three distinct types: the non-polar and non-quadrupolar (but polarizable and quadrupolarizable) Ar, Kr, Xe, and CH_4; the quadrupolar N_2, CO_2, CS_2, and C_6H_6, and the polar H_2O and CH_3OH. The analysis allows the calculation of the cavity radius and the quadrupolar length of these fluids. The following conclusions have been made:

(i) The quadrupoles in the medium affect ε measurably and accurate data for ε of a given liquid allow the quadrupolar strength of this liquid to be calculated.

(ii) In the case of quadrupolar liquids, the quadrupoles result in a weak temperature dependence of ε that is absent in Onsager's original theory.

(iii) We found that the cavity radius is a function of ρ only (except for water, probably due to the failure of our model). In several aspects, the cavity radii we calculated make better sense than Böttcher's (i.e., than those stemming from the original theory of Onsager). First, Böttcher's radii possess an artificial dependence on T that drops off when L_Q is accounted for (Figs. 5(a) and 6(a)). Second, Böttcher's radii may increase with density (Fig. 7(a))—such dependence corresponds to negative compressibility of the cavity which is unrealistic. This defect also disappears when medium's quadrupole polarizability is taken into account.

(iv) The value $L_Q = 0.81$ Å for CH_3OH calculated from our theory corresponds well with $L_Q = 1.1 \pm 0.2$ Å obtained previously from the effect of the ion-quadrupole interactions on the activity coefficient of NaBr in methanol solution.[10] The results for L_Q of CO_2 and C_6H_6 are in fair agreement with those that Jeon and Kim[8] determined from Stokes shift data. To our knowledge, there is no other model in the literature that leads to such reasonable values for the quadrupolarizability of liquids.

(v) Our model allows the parameterization of the experimental $\varepsilon(\rho,T)$ for a wide range of conditions with only 2 parameters: the coefficients k_ρ and k_0 in Eq. (57). The values listed in Table I and Eqs. (50), (53) and (57) can be used to calculate ε with extreme accuracy as a function of ρ and T: for non-polar liquids, $dev_\varepsilon = 0.0004\text{-}0.0010 \times \varepsilon_0$, approaching the experimental accuracy. The same procedure yields also the value of the macroscopic quadrupole polarizability and R_{cav}.

Let us finally discuss the limitations of the model and the routes to its development:

(i) The macroscopic theory of the quadrupole interactions has an obvious fault—the characteristic distance of the short-range quadrupole interaction is of the order of the molecular sizes so their continual description is a strong approximation. As with dipoles, this can be corrected by introducing levels of atomic description. The classical theory of Onsager for the dielectric permittivity of liquids has been largely superseded by Kirkwood's theory[43] that does that. Therefore, an obvious extension of this work is the generalization of Kirkwood's model to quadrupolar solvents. Of course, a more accurate approach is the microscopic one;[28–36] the existing works in that direction need, however, to be generalized to molecules of non-zero quadrupolarizability α_q, since it has a significant contribution to the quadrupolar strength of the liquids (50% of α_Q of CS_2 is due to the quadrupole polarizability of the molecule).

(ii) Onsager's model works well with quadrupolar liquids but faces severe problems when applied to small polar molecules such as water. We traced the main problem to the fact that the model fails to describe correctly the dielectric saturation in the vicinity of the cavity. To resolve this problem, one must use non-linear constitutive relations for $\boldsymbol{P}$ and $\mathbf{Q}$, involving also orientational dipole-quadrupole polarizability. This was done in part by Booth,[88] but his analysis is far from complete.

(iii) For most molecules, the cavity shape is different from sphere. Böttcher,[15] among others, generalized the original model of Onsager to ellipsoidal cavities. The same generalization is required for quadrupolar solvents.

Some additional discussion on the limitations of Onsager's theory is provided by Cichocki and Felderhof.[89] A contribution of our work is that it corrects Onsager's model to make it applicable to liquids made of non-polar molecules of large quadrupole moment. In the past, Onsager's model has been widely used to extract α_p and $\boldsymbol{p}_0$ from the experimental dependence $\varepsilon(\rho,T)$ of liquids.[15,41,74] Similarly, our generalization allows in principle α_q and $\mathbf{q}_0$ to be determined from $\alpha_Q(\rho,T)$ of a liquid.

The main field of application of our theory is the physical chemistry of non-polar but quadrupolar solvents—i.e., dense liquids made of molecules without permanent dipole moment. The quadrupole interactions play significant role in the properties of these liquids, especially at high pressures. The results in Sec. III B for liquid CH_4, C_6H_6, and CH_3OH are the first step toward the development and parameterization of a cavity model for solutions of polar molecules in fuels and lubricants, a problem of significant practical importance. The change of solubility of various polar and ionic substances in fuel is resulting in the formation of internal nozzle deposits,[90,91] and in crude oil—in the polar asphaltene deposits;[92] the dipole-quadrupole interactions must play an essential role in these processes. This will be demonstrated in a following study.

ACKNOWLEDGMENTS

The authors would like to acknowledge the funding and technical support from BP through the BP International Centre for Advanced Materials (BP-ICAM) which made this research possible, and to Dr. Sorin Filip who contributed to the formulation of the problem.

[1]J. D. Jackson, *Classical Electrodynamics*, 1st ed. (John Wiley & Sons, Inc., New York, 1962); *Classical Electrodynamics*, 3rd ed. (John Wiley & Sons, Inc., New York, 1999).
[2]R. E. Raab and O.L.de. Lange, *Multipole Theory in Electromagnetism* (Clarendon, Oxford, 2005).
[3]J. E. Mayer and M. G. Mayer, Phys. Rev. **43**, 605 (1933).
[4]R. A. Satten, J. Chem. Phys. **26**, 766 (1957).
[5]R. M. Sternheimer, Phys. Rev. **96**, 951 (1954).
[6]S. M. Chitanvis, J. Chem. Phys. **104**, 9065 (1996).
[7]J. Jeon and H. J. Kim, J. Chem. Phys. **119**, 8606 (2003).
[8]J. Jeon and H. J. Kim, J. Chem. Phys. **119**, 8626 (2003).
[9]R. I. Slavchov and T. I. Ivanov, J. Chem. Phys. **140**, 074503 (2014).
[10]R. I. Slavchov, J. Chem. Phys. **140**, 164510 (2014).
[11]R. I. Slavchov, I. M. Dimitrova, and T. I. Ivanov, J. Chem. Phys. **143**, 154707 (2015).
[12]R. M. Ernst, L. Wu, C.-H. Lui, S. R. Nagel, and M. E. Neubert, Phys. Rev. B **45**, 667 (1992).
[13]A. D. Buckingham, Adv. Chem. Phys. **12**, 107 (1967).
[14]L. Onsager, J. Am. Chem. Soc. **58**, 1486 (1936).
[15]C. J. F. Böttcher, *Theory of Electric Polarization* (Elsevier, Amsterdam, 1952).
[16]R. J. Abraham and M. A. Cooper, J. Chem. Soc. B **1967**, 202.
[17]J. Tomasi, B. Mennucci, and R. Cammi, Chem. Rev. **105**, 2999 (2005).
[18]C. Reichardt and T. Welton, *Solvents and Solvent Effects in Organic Chemistry* (Wiley-VCH, Weinheim, 2011).
[19]N. S. Bayliss and E. G. McRae, J. Phys. Chem. **58**, 1002 (1954).
[20]W. L. Jorgensen, J. Phys. Chem. **87**, 5304 (1983).
[21]L. Došen-Mićović and V. žigman, J. Chem. Soc., Perkin Trans. 2 **1985**, 625.
[22]M. J. Kamlet, J. L. M. Abboud, and R. W. Taft, in *Progress in Physical Organic Chemistry*, edited by R. W. Taft (Wiley, 1981), Vol. 13.
[23]K. L. Laidler and H. Eyring, Ann. N. Y. Acad. Sci. **39**, 303 (1939).
[24]K. J. Laidler, in *Chemical Kinetics* (McGraw-Hill, NY, 1950), Chap. V.
[25]R. A. Marcus, J. Chem. Phys. **24**, 966 (1956).
[26]J. B. Foresman, T. A. Keith, K. B. Wiberg, J. Snoonian, and M. J. Frisch, J. Phys. Chem. **100**, 16098 (1996).
[27]K. V. Mikkelsen, H. Ågren, H. J. A. Jensen, and T. Helgaker, J. Chem. Phys. **89**, 3086 (1988).
[28]D. V. Matyushov and G. A. Voth, J. Chem. Phys. **111**, 3630 (1999).
[29]A. A. Milischuk and D. V. Matyushov, J. Chem. Phys. **124**, 204502 (2006).
[30]A. A. Milischuk and D. V. Matyushov, J. Chem. Phys. **123**, 044501 (2005).
[31]G. N. Patey, Mol. Phys. **35**, 1413 (1978).
[32]G. N. Patey, D. Levesque, and J. J. Weis, Mol. Phys. **38**, 1635 (1979).
[33]F. O. Raineri and H. L. Friedman, Adv. Chem. Phys. **107**, 81 (1999).
[34]W. B. Streett and D. J. Tildesley, Proc. R. Soc. A **355**, 239 (1977).
[35]D. Levesque, J. J. Weis, and G. N. Patey, Mol. Phys. **51**, 333 (1984).
[36]B. Sellner and S. M. Kathmann, J. Chem. Phys. **141**, 18C534 (2014).
[37]V. V. Batygin and I. N. Toptygin, *Sbornik Zadach po Elektrodinamike i Spetzialnoy Teorii Otnositelnosti*, 4th ed. (Lan, 2010), p. 283 (in Russian).
[38]R. I. Slavchov and I. M. Dimitrova, Bulg. J. Chem. **3**, 51 (2014).
[39]M. Born, Z. Phys. **1**, 45 (1920).
[40]A. D. Buckingham, J. Chem. Phys. **30**, 1580 (1959).
[41]H. Fröhlich, *Theory of Dielectrics* (Clarendon, Oxford, 1958).
[42]J. Kongsted, A. Osted, K. V. Mikkelsen, and O. Christiansen, Chem. Phys. Lett. **364**, 379 (2002).
[43]J. G. Kirkwood, J. Chem. Phys. **7**, 911 (1939).
[44]The use of Eq. (54) for the determination of R_{cav} has the feature that it yields the Clausius-Mossotti and Lorentz-Lorenz equations as limits of main Eq. (50). Even without this assumption, at infinite dilution, the three equations have the same series of $\varepsilon(C)$ at $C \to 0$ up to $O(C^3)$.
[45]A. Passinsky, Acta Physicochim. URSS **8**, 385 (1938).
[46]J. Padova, J. Chem. Phys. **40**, 691 (1964).
[47]C.-G. Zhan and D. M. Chipman, J. Chem. Phys. **109**, 10543 (1998).
[48]Y. Luo, H. Ågren, and K. V. Mikkelsen, Chem. Phys. Lett. **275**, 145 (1997).
[49]Y. Luo, P. Norman, H. Ågren, K. O. Sylvester-Hvid, and K. V. Mikkelsen, Phys. Rev. E **57**, 4778 (1998).
[50]B. Linder and D. Hoernschemeyer, J. Chem. Phys. **46**, 784 (1967).
[51]C. J. F. Böttcher, Physica (Amsterdam) **9**, 945 (1942).
[52]P. Debye, Phys. Z. **13**, 97 (1912).
[53]A. Michels, C. A. Ten Seldam, and S. D. J. Overdijk, Physica **17**, 781 (1951).
[54]M. Lallemand and D. Vidal, J. Chem. Phys. **66**, 4776 (1977).
[55]R. L. Amey and R. H. Cole, J. Chem. Phys. **40**, 146 (1964).
[56]G. Maroulis and D. M. Bishop, J. Phys. B: At. Mol. Phys. **18**, 4675 (1985).
[57]N. E. Hill, W. E. Vaughan, A. H. Price, and M. Davies, *Dielectric Properties and Molecular Behaviour* (Van Nostrand Reinhold, London, 1969).
[58]Eq. (57) can be used to fit directly the data for R_{cav} vs. ρ in Fig. 3(a). This procedure is easy to code but it gives significant weight to the dispersed data points at small densities and thus introduces serious inaccuracies in the final results for k_0 and k_ρ, and leads to increased dev_ε.
[59]G. Maroulis and A. J. Thakkar, J. Chem. Phys. **89**, 7320 (1988).
[60]G. Maroulis, Chem. Phys. Lett. **226**, 420 (1994).
[61]*CRC Handbook of Chemistry and Physics*, edited by W. M. Haynes (CRC, New York, 2011).
[62]G. C. Straty and R. D. Goodwin, Cryogenics **13**, 712 (1973).
[63]J. F. Ely and G. C. Straty, J. Chem. Phys. **61**, 1480 (1974).
[64]G. Maroulis and A. J. Thakkar, J. Chem. Phys. **88**, 7623 (1988).
[65]G. Maroulis, Chem. Phys. **291**, 81 (2003).
[66]T. Moriyoshi, T. Kita, and Y. Uosaki, Ber. Bunsenges. Phys. Chem. **97**, 589 (1993).
[67]A. Michels and L. Kleerekoper, Physica **6**, 586 (1939).
[68]F. G. Keyes and J. G. Kirkwood, Phys. Rev. **36**, 754 (1930).
[69]F. I. Mopsik, J. Chem. Phys. **50**, 2559 (1969).
[70]G. Maroulis, Chem. Phys. Lett. **199**, 250 (1992).
[71]N. Gee, K. Shinsaka, J.-P. Dodelet, and G. R. Freeman, J. Chem. Thermodyn. **18**, 221 (1986).
[72]H. Hartmann, A. Neumann, and G. Rinck, Z. Phys. Chem. **44**, 204 (1965).
[73]J. K. Vij and W. G. S. Scaife, J. Chem. Phys. **64**, 2226 (1976).
[74]G. I. Skanavi, *Physics of Dielectrics (Weak Field Region)* (GITTL, Moscow, 1949) (in Russian).

[75]J. N. Israelachvili, *Intermolecular and Surface Forces*, 3rd ed. (Academic Press, Burlington, MA, 2011).
[76]D. P. Fernández, Y. Mulev, A. R. H. Goodwin, and J. M. H. Levelt Sengers, J. Phys. Chem. Ref. Data **24**, 33 (1995).
[77]G. S. Kell, J. Chem. Eng. Data **20**, 97 (1975).
[78]T. Grindley and J. E. Lind, Jr., J. Chem. Phys. **54**, 3983 (1971).
[79]E. R. Batista, S. S. Xantheas, and H. Jónsson, J. Chem. Phys. **109**, 4546 (1998).
[80]D. M. Bishop and J. Pipin, Theor. Chim. Acta **71**, 247 (1987).
[81]C. Huiszoon, Mol. Phys. **58**, 865 (1986).
[82]P. L. Silvestrelli and M. Parrinello, Phys. Rev. Lett. **82**, 3308 (1999).
[83]G. Åkerlöf, J. Am. Chem. Soc. **54**, 4125 (1932).
[84]V. A. Rana, H. Chaube, and D. H. Gadani, J. Mol. Liq. **164**, 191 (2011).
[85]R. D. Bezman, E. F. Casassa, and R. L. Kay, J. Mol. Liq. **73-74**, 397 (1997).
[86]E. Schadow and R. Steiner, Z. Phys. Chem. **66**, 105 (1969).
[87]T. Sun, S. N. Biswas, N. J. Trappeniers, and C. A. Ten Seldam, J. Chem. Eng. Data **33**, 395 (1988).
[88]F. Booth, J. Chem. Phys. **19**, 391 (1951).
[89]B. Cichocki and B. U. Felderhof, J. Chem. Phys. **92**, 6104 (1990).
[90]R. Caprotti, A. Breakspear, O. Graupner, T. Klaua, and O. Kohnen, SAE 2006-01-3359, 2006.
[91]A. Tanaka, K. Yamada, T. Omori, S. Bunne, and K. Howokawa, SAE 2013-01-2661, 2013.
[92]J. G. Speight, *The Chemistry and Technology of Petroleum*, 5th ed. (CRC Press, 2014).
[93]See supplementary material at http://dx.doi.org/10.1063/1.4943196 for the following. Section A: Solving the quadrupolar Coulomb-Ampère law. Section B: Average quadrupole moment per molecule and derivation of the equation for α_Q. Section C: Average molecular quadrupolarizability vs. components of the molecular quadrupole polarizability tensor. Section D: Sample Maple code for solving Eqs. (50) and (53) for L_Q and R_{cav}.